

Interference underlies attenuation upon relearning in sensorimotor adaptation

Short title: Interference of sensorimotor memories

Guy Avraham* and Richard B Ivry

Department of Psychology and Helen Wills Neuroscience Institute, University of California,
Berkeley, Berkeley, CA 94720, USA

* Corresponding author

E-mail: guyavraham@berkeley.edu

1 Abstract

2 Savings refers to the gain in performance upon relearning a task. In sensorimotor adaptation,
3 savings is tested by having participants adapt to perturbed feedback and, following a washout
4 block during which the system resets to baseline, presenting the same perturbation again. While
5 savings has been observed with these tasks, we have shown that the contribution from implicit
6 sensorimotor adaptation, a process that uses sensory prediction errors to recalibrate the
7 sensorimotor map, is actually attenuated upon relearning (Avraham et al., 2021). In the present
8 study, we test the hypothesis that this attenuation is due to interference arising from the
9 washout block, and more generally, from experience with a different relationship between the
10 movement and the feedback. In standard adaptation studies, removing the perturbation at the
11 start of the washout block results in a salient error signal in the opposite direction to that
12 observed during learning. As a starting point, we replicated the finding that implicit adaptation is
13 attenuated following a washout period in which the feedback now signals a salient opposite
14 error. When we eliminated visual feedback during washout, implicit adaptation was no longer
15 attenuated upon relearning, consistent with the interference hypothesis. Next, we eliminated the
16 salient error during washout by gradually decreasing the perturbation, creating a scenario in
17 which the perceived errors fell within the range associated with motor noise. Nonetheless,
18 attenuation was still prominent. Inspired by this observation, we tested participants with an
19 extended experience with veridical feedback during an initial baseline phase and found that this
20 was sufficient to cause robust attenuation of implicit adaptation during the first exposure to the
21 perturbation. This effect was context-specific: It did not generalize to movements that were not
22 associated with the interfering feedback. Taken together, these results show that the implicit
23 sensorimotor adaptation system is highly sensitive to memory interference from a recent
24 experience with a discrepant action-outcome contingency.

25 **Introduction**

26 People exhibit a remarkable ability to retain motor skills. The skier finds herself performing close
27 to her previous level of competence after an 8-month layoff and, while the mind might be wary,
28 our bodies are able to readily recall how to ride a bike even if they have not done so for many
29 years. Indeed, laboratory studies of retention have highlighted the phenomenon of savings, the
30 benefit in performance observed when relearning a previously acquired skill. Originally
31 described in the verbal learning domain (Ebbinghaus, 1913), savings has since come to be
32 recognized as a rather ubiquitous phenomenon, including many examples in the motor learning
33 literature (Coltman et al., 2019; Doyon et al., 2009; Kojima et al., 2004; Mawase et al., 2014;
34 Medina et al., 2001; Milner, 1962; Walker et al., 2002).

35 Sensorimotor adaptation tasks have provided an interesting testbed for exploring
36 savings in motor learning. In visuomotor adaptation, feedback indicating the participant's hand
37 position is perturbed, usually by imposing an angular rotation. Participants learn to compensate,
38 reaching in the opposite direction of the perturbation. Savings is tested by presenting the same
39 perturbation over two learning blocks, separated by a washout phase with non-perturbed
40 feedback (Albert et al., 2022; Herzfeld et al., 2014; Huang et al., 2011; Krakauer, 2009;
41 Krakauer et al., 2005; Zarahn et al., 2008). With this design, participants often exhibit savings,
42 showing a higher rate of adaptation during the second learning block.

43 In line with the common conception about the procedural nature of motor skills, this form
44 of savings has been hypothesized to reflect changes in an implicit system that serves to keep
45 the sensorimotor system well-calibrated (Albert et al., 2022, 2021; Coltman et al., 2019;
46 Hadjiosif et al., 2023; Yin and Wei, 2020). For example, it has been proposed that the sensitivity
47 of this system is enhanced when participants are exposed to errors during initial learning,
48 resulting in faster learning upon re-exposure to similar errors (Albert et al., 2021; Herzfeld et al.,
49 2014).

50 However, by using methods that isolate the contribution of this recalibration process, we
51 have found that implicit sensorimotor adaptation is actually attenuated during relearning
52 (Avraham et al., 2021; see also Hamel et al., 2022, 2021; Leow et al., 2020; Stark-Inbar et al.,
53 2016; Tsay et al., 2021b; Wang and Ivry, 2023; Yin and Wei, 2020). Savings, when observed in
54 adaptation tasks, appears to largely reflect the operation of other learning processes such as
55 the recall of a successful explicit strategy (Avraham et al., 2021; Haith et al., 2015; Huberdeau
56 et al., 2019; Morehead et al., 2015).

57 Why does implicit sensorimotor adaptation show attenuated relearning rather than
58 savings? We can consider two hypotheses. The first hypothesis is also based on the idea that
59 exposure to a given error changes the sensitivity of the system in response to that error when
60 re-encountered. However, rather than increasing with familiarity, sensitivity may decrease with
61 familiarity. That is, the adaptation system becomes less responsive after prolonged exposure to
62 an error. Mechanistically, desensitization could arise from a saturation of recently activated
63 synapses (Hamel et al., 2022, 2021; Nguyen-Vu et al., 2017).

64 An alternative hypothesis is based on the idea of interference, a classical concept in the
65 psychological memory literature (Underwood, 1957). In the typical design of a savings study, the
66 first block with perturbed feedback is followed by a washout block with veridical feedback to
67 reset the behavior back to baseline. When exposed to veridical feedback in the adapted state,
68 the participant experiences an error in the opposite direction of that experienced during the
69 initial learning block. Thus, at the end of the washout block, the participant has been exposed to
70 two error signals of opposite signs, one associated with the initial perturbation and a second
71 associated with the washout. When the perturbation is re-introduced, memories associated with
72 these two error signals may compete with one another (Bouton, 1986), especially given that the
73 context is similar (reaching to the same target). As such, the response to the re-introduced

74 perturbation may be attenuated due to interference from the association established during the
75 washout block.

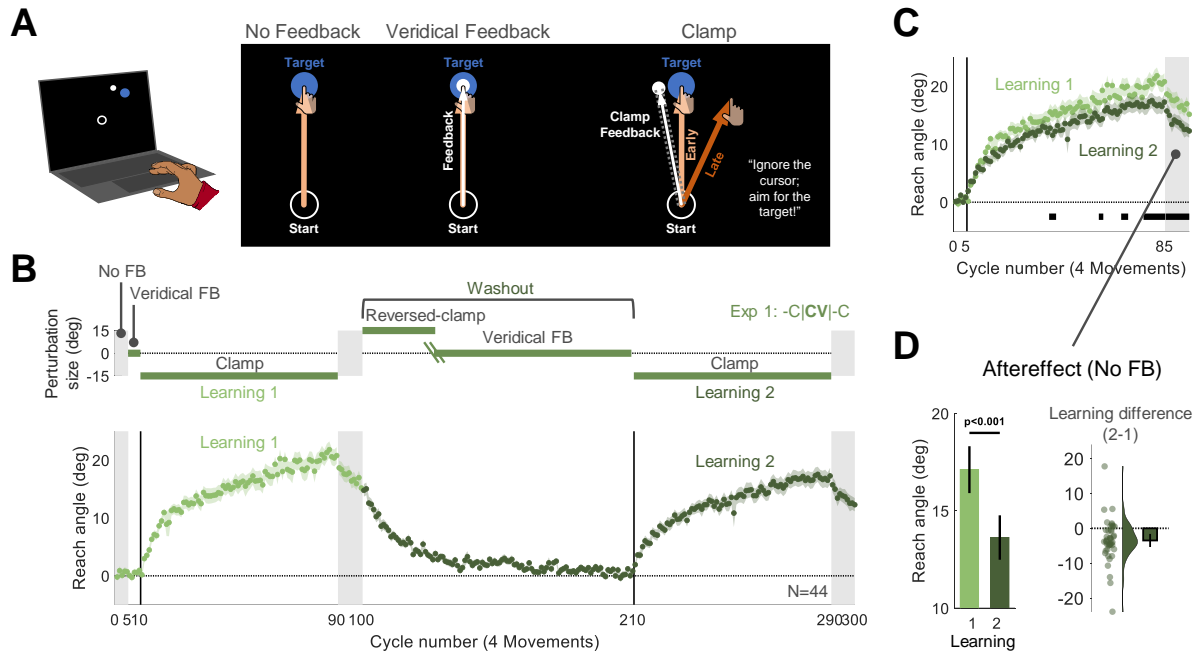
76 We evaluate these two hypotheses in a series of behavioral experiments.

77

78 **Results**

79 We employed a visuomotor task in which task-irrelevant clamped feedback was used to isolate
80 implicit adaptation (Morehead et al., 2017) (Fig. 1A). In this task, participants reach to a visual
81 target while the cursor follows a path with a fixed angular offset from the target (e.g., by 15°).
82 Despite instructions to ignore the cursor, participants show robust implicit adaptation to this type
83 of perturbation, with the direction of the hand movement (reach angle) gradually shifting away
84 from the target (and cursor). In our previous study, we used this manipulation over two learning
85 blocks that were separated by a washout block and found that the implicit change in reach angle
86 during the second learning block was attenuated with respect to the first learning block
87 (Avraham et al., 2021).

88 In Experiment 1, we aimed to replicate this attenuation effect using a similar relearning
89 protocol (abbreviated as -C|CV|-C, Fig. 1B). There were two learning blocks with -15° clamped
90 feedback (-C), separated by a washout block. The washout block started with reversed clamped
91 feedback, with the cursor now shifted in the opposite direction (15°, C). This was expected to
92 implicitly drive the adapted hand movements back towards the target. Once the participant's
93 reaches were near the target, we transitioned to veridical feedback (V) for the remainder of the
94 washout block. In this manner, the average reach angle at the start of the two clamp blocks
95 should be similar. We also included a short no-feedback block after each learning block to
96 assess the aftereffect. During all phases of the experiment, the instructions remained the same:
97 Reach directly to the target.



98

99 **Fig 1. Experiment 1: Upon relearning a visuomotor rotation, implicit adaptation is attenuated.**

100 (A) Task design and schematics of all trial types in Experiment 1. Using a trackpad or mouse, participants
101 ($N=44$) moved a cursor from the start location (white circle) to a target (blue disk), with the target
102 appearing at one of four locations (one representative location is depicted). There were 3 types of trials:
103 1) No feedback, with the cursor disappearing at movement onset; 2) Veridical feedback, in which the
104 direction of the cursor (small white disk) was veridical with respect to the direction of the movement; 3)
105 Clamped feedback, in which the cursor followed an invariant path with respect to the target. (B) Top:
106 Experimental protocol. The $-C|CV|-C$ abbreviation indicates the main block-level structure of the
107 experiment. There were two learning blocks with clamped feedback (-C), each followed by an aftereffect
108 block with no feedback. To reset the sensorimotor map following the first learning block, we used a
109 washout block composed of a reversed-clamp feedback phase (C) and a veridical feedback phase (V).
110 The green oblique lines in the washout block mark the transition between the two phases, with the length
111 of the reversed clamp phase determined on an individual basis (see Methods). Bottom: Time course of
112 mean reach angle, with the data averaged within each cycle of four movements. Light and dark shading
113 signify learning blocks 1 and 2, respectively, with the onset of the clamped feedback marked by the
114 vertical solid lines. (C) Overlaid reach angle functions for the two learning blocks and two aftereffect

115 blocks. Horizontal thick black lines denote clusters that show a significant difference between blocks 1
116 and 2 ($p < 0.05$). (D) The left panel (pair of bars) presents the aftereffect data (mean \pm SEM) for each
117 learning block, measured as the averaged reach angle across all cycles in each aftereffect block. The
118 right panel shows the within-participant difference (Aftereffect 2 – Aftereffect 1; dots and violin plot-
119 distribution of individual difference scores, bar- mean difference and 95% CI). SEM, standard error of the
120 mean. CI, Confidence Interval.

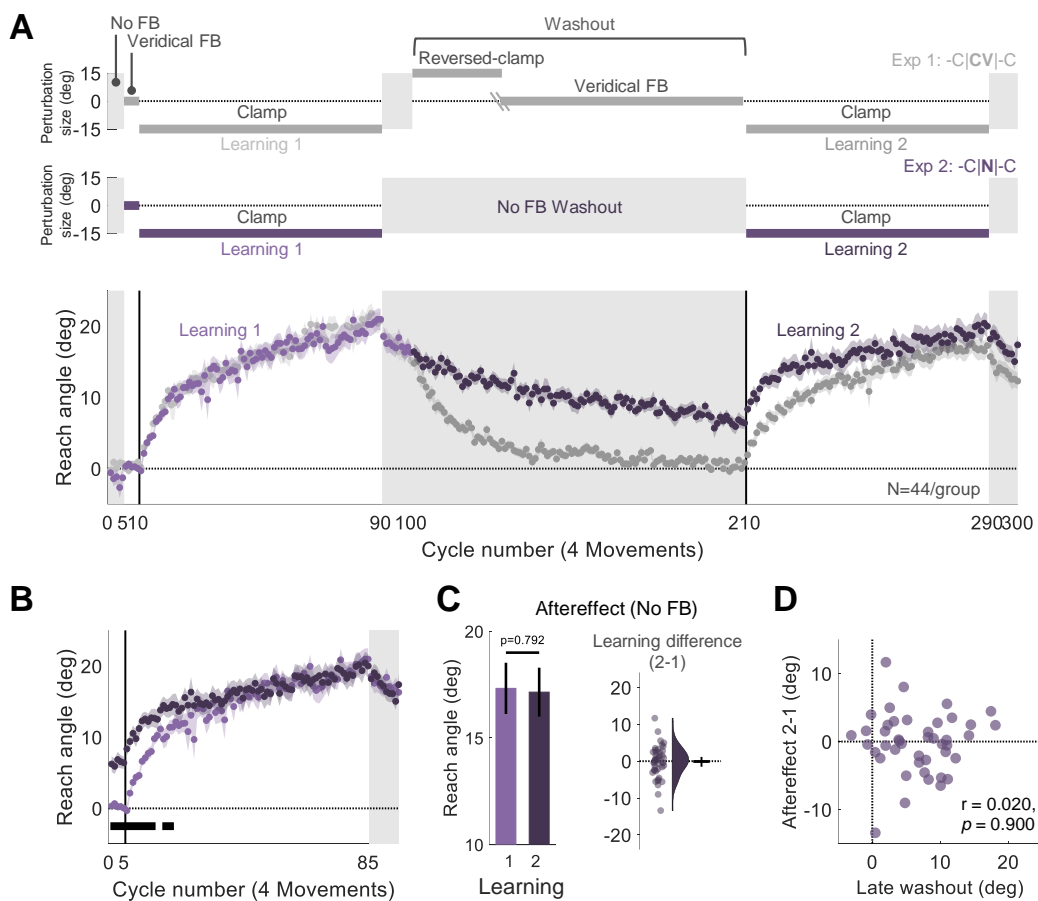
121

122 Participants exhibited robust adaptation during the first learning block, and their behavior
123 reverted back to baseline during the washout block. Consistent with our previous findings, the
124 overall implicit change in reach angle during the second learning block was smaller than during
125 the first learning block (Figs. 1B, 1C). To evaluate this effect statistically, we compared the
126 reach angle between the first and second learning blocks, averaging the data over cycles of four
127 reaches (one reach per target). We used a non-parametric cluster-based permutation test to
128 identify clusters of cycles that differed between the two learning blocks (Avraham et al., 2021;
129 Labruna et al., 2019; Maris and Oostenveld, 2007). This analysis revealed multiple clusters in
130 which there was a decrease in reach angle during the second learning block. In line with the
131 cluster-based results, attenuation was also significant when the analysis was restricted to the
132 aftereffect measure of adaptation, namely the mean reach angle during the aftereffect blocks
133 ([mean difference, 95% CI], -3.48° , $[-5.36^\circ - 1.61^\circ]$, $t(43) = -3.75$, $p = 5.20 \times 10^{-4}$, $BF_{10} = 53.2$, $d =$
134 -0.57 , Fig. 1E).

135 In Experiment 1, relearning was tested after a washout block in which participants had
136 performed 110 reaches to each target in the presence of feedback – either reversed-clamp or
137 veridical – that was different than the error signal that drove initial learning. It is unclear if the
138 attenuation is due to the exposure to these alternative and potentially interfering forms of
139 feedback or reflects desensitization to the original error. Experiment 2 was designed to address

140 this question. As in Experiment 1, participants experienced two learning blocks that were
141 separated by a washout block (Fig. 2A). However, no feedback was presented during the entire
142 110-cycle washout block (-C|N|-C design). If attenuation upon relearning is due to interference
143 from the feedback experienced during washout, removing this feedback should rescue
144 attenuated learning. In contrast, if attenuation is driven by desensitization to a familiar error, we
145 should again observe attenuation in the second learning block following the no-feedback
146 washout block.

147



148

149 **Fig 2. Experiment 2: Implicit adaptation is not attenuated upon relearning when feedback is**
150 **eliminated during the washout block.**

151 (A) Experimental protocol and learning functions. Top: Participants (N=44) experienced 110 cycles of
152 trials without feedback (N) during a washout block that separated the two learning blocks (-C|N|-C design,
153 purple). Bottom: Time course of mean reach angle averaged over cycles. Light and dark shading signify
154 learning blocks 1 and 2, respectively, with the onset of the clamped feedback marked by the vertical solid
155 lines. The design and learning functions from Experiment 1 are reproduced here to provide a visual point
156 of comparison (gray). (B) Overlaid reach angle functions for the two learning blocks and two aftereffect
157 blocks in Experiment 2 (significant clusters based on $p < 0.05$) (C) The left panel presents the aftereffect
158 (mean \pm SEM) for each learning block and the right panel the within-participant difference (Aftereffect 2 –
159 Aftereffect 1; dots and violin plot- distribution of individual difference scores, bar- mean and 95% CI). (D)
160 Scatter plot showing no relationship between the reach angle at late washout and change in relearning
161 (Aftereffect 2 – Aftereffect 1). SEM, standard error of the mean. CI, Confidence Interval.

162

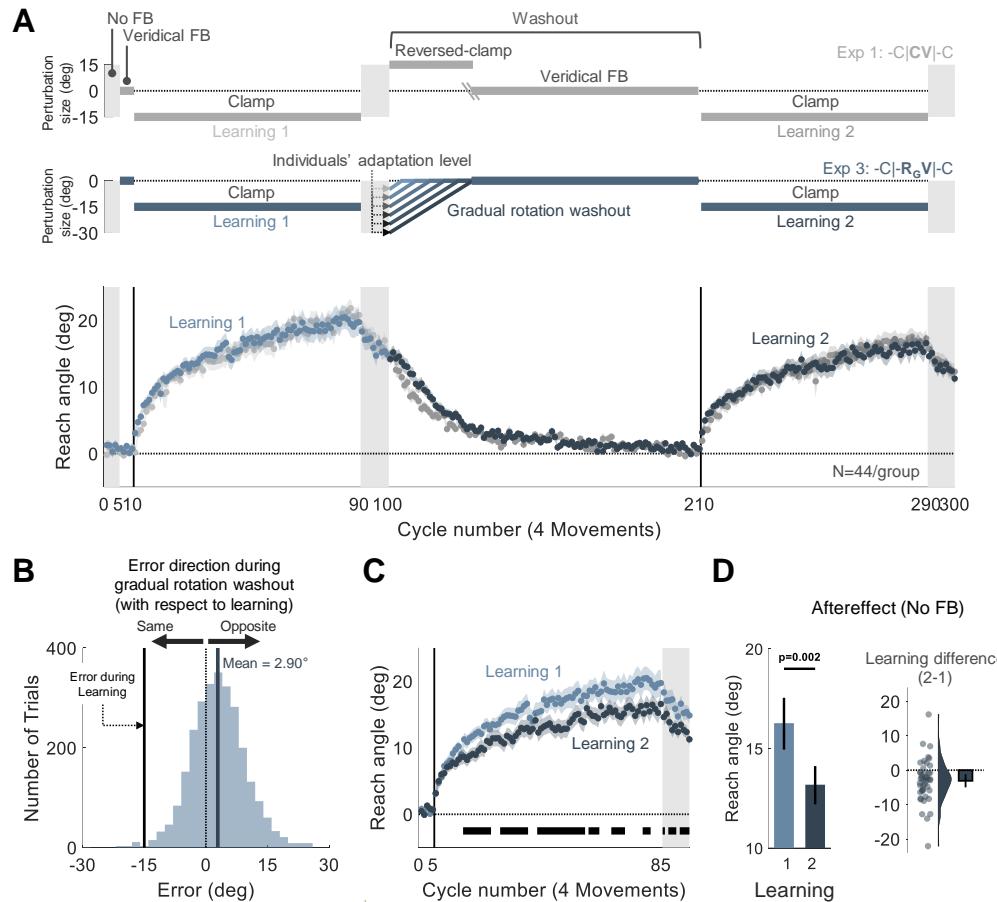
163 Despite the absence of feedback, adaptation slowly decayed throughout the washout
164 block, presumably due to some form of forgetting or attraction to the original state of the
165 sensorimotor system (Fig. 2A). The decay was, on average, incomplete by the end of the
166 washout block. Thus, the mean reach angle at the beginning of the second learning block was
167 higher than at the start of the first Learning block (Fig 2B). However, after ~20 cycles, the two
168 functions converged and reached a similar state of adaptation by the end of the clamp blocks.
169 Thus, we failed to observe attenuation. This null result was confirmed in the analysis of the
170 aftereffect data (-0.18° , $[-1.52^\circ \ 1.16^\circ]$, $t(43) = -0.266$, $p = 0.792$, $BF_{10} = 0.169$, $d = -0.04$, Fig.
171 2C). Interestingly, the difference between reach angle in the first and second aftereffect blocks
172 was unrelated to the extent of decay observed during the washout block ($r = 0.020$, $p = 0.900$,
173 $BF_{10} = 0.12$). As can be seen in Figure 2D, even those participants who showed complete
174 washout in the absence of feedback did not exhibit attenuated relearning.

175 In summary, the results of Experiment 2 indicate that attenuation upon relearning is not
176 due to desensitization to the error that participants experienced during initial learning. Rather,

177 the results are consistent with the hypothesis that attenuation is due to interference that arises
178 from the feedback experienced during the washout block.

179 What conditions might produce interference during relearning? With the introduction of
180 the reversed clamp at the beginning of the washout block in Experiment 1, participants are
181 exposed to a large error signal that is in the opposite direction to that experienced during the
182 initial learning block. Interference may arise from a competition between the memory traces
183 associated with the two opposing error signals (Heald et al., 2021; Sing and Smith, 2010). This
184 hypothesis can account for the results of Experiment 2 since there was no error presented
185 during the washout block. An even stronger test would be to use feedback during the washout
186 block that did not provide salient error information that was opposite to that observed during the
187 initial learning block.

188 We implemented this test in Experiment 3. Following implicit adaptation with the rotated
189 clamped feedback, participants were told at the start of the washout block that the cursor would
190 now be aligned with their hand. However, we actually applied a visuomotor rotation that was
191 contingent on the movement direction of the hand, setting the size of the rotation so that the
192 cursor would move close to the target (see Methods). The size was determined on an individual
193 basis: For example, if the participant had adapted 19° in the clockwise direction at the end of the
194 rotation block, the rotation was initially set to 19° in the counterclockwise direction. This
195 perturbation was gradually reduced over the washout block (Fig. 3A). Gradual changes in the
196 magnitude of a visuomotor rotation have been shown to result in pronounced implicit adaptation
197 (Christou et al., 2016; Modchalingam et al., 2023). Here, we used this method to nullify an
198 adapted state. When the size of the rotation had decreased to 0°, the feedback was veridical
199 and remained so for the rest of the washout block. We assumed that this method would
200 minimize the participant's experience with salient opposite-signed errors during the early (and
201 all) stages of the washout block despite having adapted during the initial learning block.



202

203 **Fig 3. Experiment 3: Attenuated adaptation does not require experience with salient, opposite
204 signed error at the beginning of washout.**

205 (A) Experimental protocol and learning functions. Top: At the beginning of the washout block in
206 Experiment 3, participants (N=44) experienced a rotated cursor that was contingent on the direction of
207 their hand movement, with the magnitude of the perturbation set to their final adaptation level at the end
208 of the first learning block; in this way, the cursor position would be near the target. The size of the rotation
209 was gradually decreased until reaching 0°, at which point it was veridical and remained so for the rest of
210 the washout block (-C|R_GV|-C design, blue). Bottom: Time course of mean reach angle averaged over
211 cycles (4 movements). Light and dark shading signify learning blocks 1 and 2, respectively, with the onset
212 of the clamped feedback marked by the solid vertical lines. The design and learning functions from
213 Experiment 1 are reproduced here to provide a visual point of comparison (gray). (B) Distribution of errors
214 experienced during the non-zero rotation phase of the washout block. These errors were small in

215 magnitude (mean=2.9°, dark blue solid line) and in the opposite direction of the error experienced during
216 the initial learning block (black solid line). Presumably, these opposite errors are the signals that drive the
217 washout of the initial adaptation. The dotted line represents zero error. **(C)** Overlaid reach angle functions
218 for the two learning blocks. Horizontal thick black lines denote clusters that show a significant difference
219 between blocks 1 and 2 ($p < 0.05$). **(D)** The left panel presents the aftereffect (mean \pm SEM) for each
220 learning block and the right panel the within-participant difference (Aftereffect 2 – Aftereffect 1; dots and
221 violin plot- distribution of individual difference scores, bar- mean and 95% CI). SEM, standard error of the
222 mean. CI, Confidence Interval.

223

224 After adaptation, participants exhibited a gradual reversion of reach angle back to
225 baseline (Fig. 3A). This washout function was somewhat slower than that observed in
226 Experiment 1 where we had used a salient, reversed clamp to achieve washout (Fig. S1),
227 presumably because the experienced errors during the initial washout trials were much smaller
228 and of variable sign in Experiment 3 ([mean \pm standard deviation], 2.90° \pm 10.1°, Fig. 3B)
229 (Avraham et al., 2020; Kim et al., 2018; Tsay et al., 2021a; Wei and Kording, 2009).

230 Contrary to our prediction, the elimination of salient, opposite-signed errors did not
231 abolish the attenuation effect. Robust attenuation was observed across the second learning
232 block and during the aftereffect block ([mean aftereffect difference, 95% CI], -3.09°, [-4.99° -
233 1.18°], $t(43) = -3.27$, $p = 0.002$, $BF_{10} = 15.11$, $d = -0.49$, Figs. 3C, 3D).

234 While the results indicate that attenuation does not require a salient change in the error,
235 an analysis of the feedback provided at the beginning of the washout block shows that
236 participants experienced opposite-signed errors more often than same-signed errors (Fig 3B.
237 Fig S2 provides a comparison with the error distribution experienced with veridical feedback).
238 The small skew in the distribution might be sufficient to produce interference.

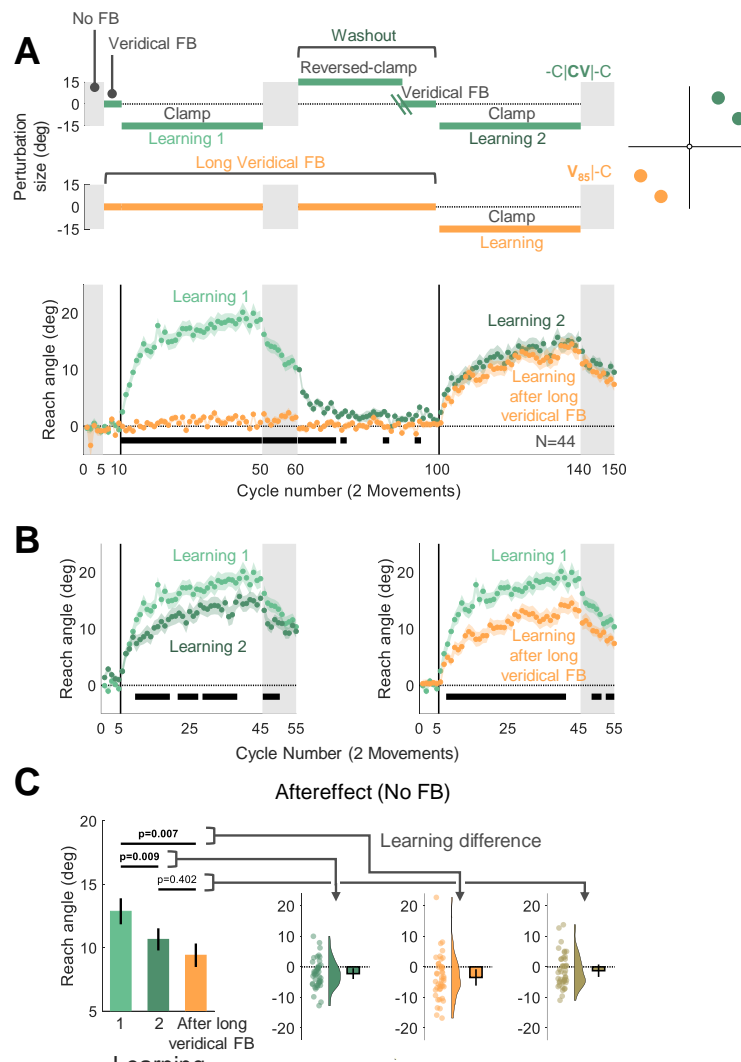
239 Alternatively, interference may arise when multiple associations are linked to the same
240 action. Up to this point, we had assumed that interference would occur when a given action
241 (e.g., moving to a given target location) was associated with two types of perturbations,
242 specifically, opposing visuomotor errors. However, simply experiencing a change in the
243 feedback, even from one that is not perturbed, may be sufficient to elicit interference.

244 We tested this hypothesis in Experiment 4 using a protracted block with veridical
245 feedback, asking if this would attenuate subsequent adaptation to a perturbation. On each trial,
246 the target appeared within one of two 30°-wide wedges located at opposite poles of the
247 workspace (~180° separation, Fig. 4A). When the target appeared in one of the wedges, the
248 perturbation followed a similar schedule to Experiment 1: Two learning blocks with clamped
249 feedback were separated by a washout block -C|CV|-C. When the target appeared in the other
250 wedge, the feedback was veridical for the first 85 cycles, followed by a single learning block with
251 clamped feedback (V₈₅|-C). Previous work has shown negligible generalization of adaptation for
252 locations separated by more than 45° (Krakauer et al., 2000; McDougle et al., 2017; Morehead
253 et al., 2017). As such, this within-participant design allowed us to ask if extended exposure to
254 veridical feedback was sufficient to attenuate adaptation. Specifically, we asked if adaptation to
255 targets in the V₈₅|-C location would be attenuated with respect to the first learning block in the -
256 C|CV|-C location.

257 For the -C|CV|-C location, adaptation in the second learning block was attenuated with
258 respect to the first learning block, consistent with the results of Experiment 1 (Fig. 4A, 4B).
259 Critically, adaptation in the V₈₅|-C location was also attenuated relative to the first learning block
260 in the -C|CV|-C location, and it was comparable to the second learning block in the -C|CV|-C
261 location. This pattern was also evident in the aftereffect data ($F[1.59, 68.5] = 7.96, p = 0.002$,
262 $BF_{10}=40.95$, and $\eta_p^2=0.16$, mean difference Aftereffect 2 – Aftereffect 1: -2.21° , 95% CI: $[-3.97^\circ$ –
263 $0.45^\circ]$, p_B {Bonferroni corrected p value} = 0.009, mean difference Aftereffect after long baseline

264 – Aftereffect 1: -3.46° , 95% CI: $[-6.14^\circ \text{ } -0.79^\circ]$, $p_B = 0.007$, mean difference Aftereffect after long
265 baseline – Aftereffect 2: -1.25° , 95% CI: $[-3.29^\circ \text{ } 0.79^\circ]$, $p_B = 0.402$, Fig. 4C). Thus, attenuation of
266 implicit adaptation does not require experience with an opposing perturbation; rather, it can also
267 arise following extended experience with veridical feedback.

268



269

270 **Fig 4. Experiment 4: Adaptation is attenuated for movements that were previously associated with**
271 **either washout after learning or an extended baseline experience with veridical feedback.**

272 **(A)** Experimental protocol and learning functions. Top: The target appeared at one of four locations, with
273 two locations falling within one 30°-wedge and the other two falling within a same-size wedge on the
274 opposite side of the workspace. Participants (N=44) experienced a -C|CV|-C schedule (cyan) in one
275 wedge and a V₈₅-C design schedule in the other wedge (orange). For the latter, the number of veridical
276 feedback cycles (85) matched the total number of cycles before relearning at the other wedge (excluding
277 the no-feedback trials). Bottom: Time course of mean reach angle averaged over cycles, with each cycle
278 consisting of 2 movements for each wedge. Light and dark cyan signify learning blocks 1 and 2 in the -
279 C|CV|-C condition. **(B)** Overlaid reach angle functions comparing the first learning block in -C|CV|-C to
280 that of the second learning block in the same wedge (left panel) and to the post long-baseline learning
281 block at the other wedge (right panel). Horizontal thick black lines (B) and (C) denote clusters that show a
282 significant difference between the functions (with $p < 0.017$ as a significance criterion, see Methods). **(C)**
283 Left panel (bars) presents the aftereffect data (mean \pm SEM) for each learning block and the right panel
284 shows the within-participant differences for three contrasts: 1) Aftereffect 2 – Aftereffect 1; 2) Aftereffect
285 after long baseline – Aftereffect 1; 3) Aftereffect after long baseline – Aftereffect 2. Dots and violin plots
286 show the distribution of individual difference scores; bar- mean and 95% CI. SEM, standard error of the
287 mean. CI, Confidence Interval.

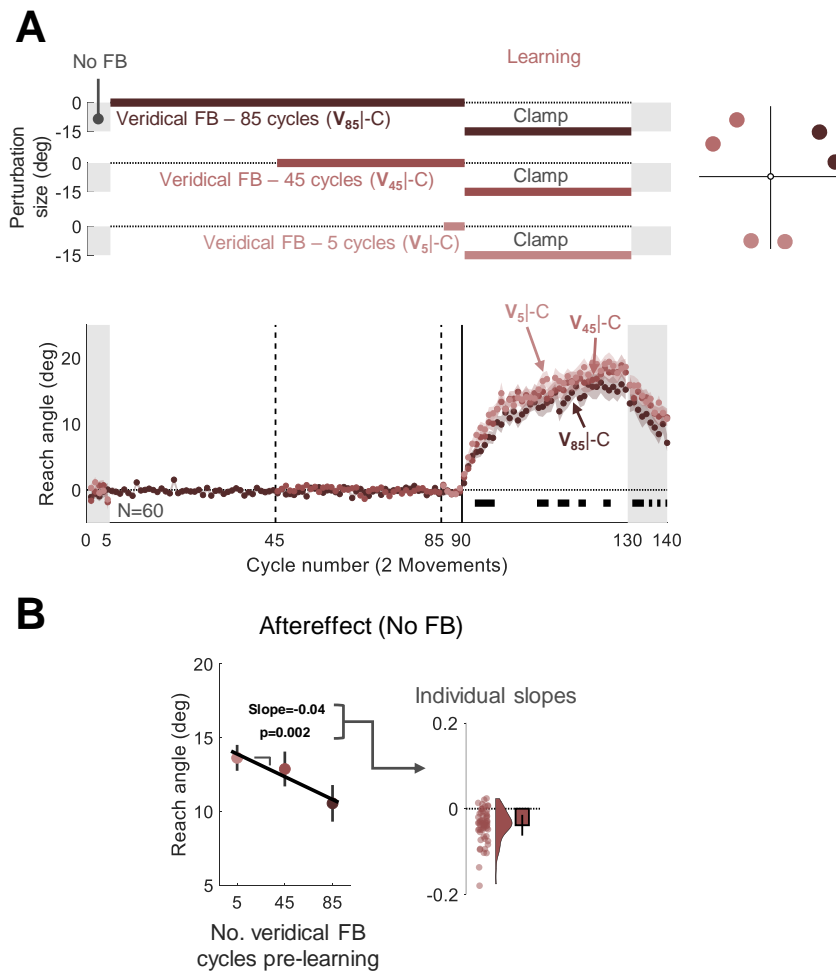
288

289 Experiment 4 was designed based on the assumption that the mechanisms underlying
290 attenuation do not generalize across the workplace. Although it is well-established that implicit
291 adaptation shows minimal generalization between regions separated by more than 45°
292 (Krakauer et al., 2000; McDougle et al., 2017; Morehead et al., 2017), generalization rules may
293 be different for attenuation. For example, if attenuation generalizes broadly, the reduced rate of
294 learning following extended exposure to veridical feedback at one wedge could be due to
295 interference arising from exposure to the reversed clamp at the other wedge.

296 Given this concern, we used an alternative design in Experiment 5 to assess the effect
297 of extended experience with veridical feedback on attenuation. The target appeared in one of

298 three wedges, with each wedge separated by at least 90° from the other two (Fig. 5A). In all
299 three wedges, there was a single learning block with clamped feedback, with the direction of the
300 perturbation the same across wedges. We varied the number of veridical feedback cycles that
301 preceded the clamped feedback block, using 5 cycles for one wedge ($V_{5|C}$), 45 cycles for a
302 second wedge ($V_{45|C}$), and 85 cycles for the third wedge ($V_{85|C}$). If experience with veridical
303 feedback is sufficient to cause interference in a context-specific manner, we expect that the
304 level of adaptation will be inversely related to the number of veridical cycles.

305



306

307 **Fig 5. Experiment 5: Interference from veridical feedback is context-specific.**

308 (A) Experimental protocol and learning functions. Top: During the learning block, participants (N=60)
309 experienced rotated clamped feedback while reaching to six targets, with two targets falling within each of
310 three wedges distributed across the workspace. For each wedge, participants experienced a different
311 number of cycles with veridical feedback prior to the learning block: 5 ($V_{5|C}$, light red); 45 ($V_{45|C}$,
312 medium red); 85 ($V_{85|C}$, dark red). Bottom: Time course of mean reach angle averaged over cycles (2
313 movements) for each wedge. The vertical solid lines at cycles 45 and 85 mark the onset of movements to
314 an additional location, and the vertical solid lines at cycles 90 mark the onset of the task-irrelevant
315 clamped feedback. Horizontal thick black lines denote clusters of cycles that show a significant
316 relationship between the reach angle and the number of veridical cycles ($p < 0.05$). (B) Left panel
317 presents the aftereffect results (mean \pm SEM) for each learning condition with the fixed effect regression
318 line obtained using a linear mixed model. Right panel shows the distribution (dots and violin plots) of
319 individuals' slopes (random effect); bar- mean slope and 95% CI. SEM, standard error of the mean. CI,
320 Confidence Interval.

321

322 The results were consistent with this prediction. A nonparametric permutation test
323 identified significant cycles during the learning and aftereffect blocks for which the reach angle
324 was negatively associated with the number of veridical cycles (Fig. 5A). This was also evident in
325 a linear mixed-effect analysis assessing the change in aftereffect across the three conditions
326 (Fixed effect slope: -0.04, [-0.06 -0.01], $t(178) = -3.14$, $p = 0.002$, Fig. 5B). Overall, the results
327 of Experiment 5 provide strong evidence that extended experience with veridical feedback can
328 interfere with implicit adaptation in a context-specific manner.

329

330 Discussion

331 Relearning paradigms have offered an important approach to studying learning and memory.
332 While many studies have demonstrated savings, indicative of latent retention of information that

333 was acquired in the past, implicit sensorimotor adaptation exhibits attenuation upon re-exposure
334 to a previously learned perturbation (Avraham et al., 2021; Hamel et al., 2022, 2021; Leow et
335 al., 2020; Stark-Inbar et al., 2016; Tsay et al., 2021b; Yin and Wei, 2020). The goal of this paper
336 was to identify the mechanisms underlying this attenuation. The results indicate that attenuation
337 is observed when an action has been associated with discrepant forms of visual feedback,
338 creating interference between two sensorimotor memories.

339

340 *Implicit adaptation is subject to interference from discrepant feedback signals*

341 In the adaptation literature, studies of relearning have typically used a design in which a
342 washout, perturbation-free block is employed between two learning blocks (Herzfeld et al.,
343 2014; Huang et al., 2011; Leow et al., 2012). The purpose of the washout block is to bring
344 behavior back to baseline (i.e., the hand movement is directed to the visual target) before the
345 re-introduction of the perturbation. As such, one can compare two learning functions that start,
346 at least superficially, from a common state. When considering overall performance, savings is
347 typically observed: Learning in the second perturbation block is faster than during the initial
348 perturbation block.

349 However, the observed behavior likely reflects the operation of multiple learning
350 processes. In particular, in addition to an implicit recalibration process, participants may employ
351 an explicit strategy to compensate for the perturbation (Bond and Taylor, 2015; Kim et al., 2021;
352 Taylor et al., 2014). Savings upon re-exposure to a perturbation appears to reflect the recall of a
353 strategy that had proven to be successful in the initial perturbation block (Avraham et al., 2021;
354 Haith et al., 2015; Morehead et al., 2015). By using non-contingent, clamped feedback, we were
355 able to eliminate strategy use and thus, by inference, isolate learning to just that produced by
356 implicit adaptation (Morehead et al., 2017; Tsay et al., 2020b). Under such conditions,

357 relearning is attenuated rather than facilitated. Critically, this attenuation has also been
358 observed in tasks that used other methods to isolate implicit sensorimotor adaptation (Avraham
359 et al., 2021; Hamel et al., 2021; Huberdeau et al., 2019; Leow et al., 2020; Yin and Wei, 2020).

360 Our initial hypothesis was that this attenuation reflects interference that arises when a
361 movement is associated with conflicting error signals. When veridical feedback is re-introduced
362 in the washout block, a salient error is experienced, one that is in the opposite direction of that
363 experienced during the initial perturbation block. Similarly, conflicting error signals are
364 associated with the same movement when reversed clamped feedback is used to drive
365 washout. Consistent with the interference hypothesis, relearning was not attenuated when
366 feedback was omitted from the washout block. However, subsequent experiments showed that
367 interference does not require conflicting error signals: We also observed attenuation when we
368 used a procedure to wash out adaptation in the absence of a salient opposite error signal and,
369 more dramatically, during an initial perturbation block that followed an extended baseline block
370 with veridical feedback. Thus, interference appears to be between discrepant feedback signals
371 and not competing error signals.

372 The attenuating effect from a prolonged baseline period with veridical feedback also
373 helps clarify that the effect is due to anterograde interference rather than retrograde interference
374 (see also Hinder et al., 2007; Krakauer et al., 2005; Miall et al., 2004; Villalba et al., 2015).
375 Anterograde interference refers to the disruptive effect of one memory on the ability to either
376 acquire or recall another memory. In contrast, retrograde interference refers to the disruptive
377 effect of a new memory on the consolidation of a previously learned memory. The fact that
378 attenuation is seen in the initial exposure to a perturbation is consistent with an anterograde
379 interference account. We recognize that retrograde interference may also be operative in the
380 experiments that included two learning blocks (Experiments 1-4). To assess this, future
381 experiments with clamped feedback could adopt classic manipulations used to evaluate the

382 relative contribution of anterograde and retrograde interference such as varying the delay
383 between the initial learning block, washout block, and re-learning block. These manipulations
384 would also be important to ask how interference effects are modulated when there is greater
385 time for consolidation of the memory associated with the initial perturbation (Bock et al., 2001;
386 Brashers-Krug et al., 1996; Caithness et al., 2004; Criscimagna-Hemminger and Shadmehr,
387 2008; Goedert and Willingham, 2002; Krakauer et al., 1999; Shadmehr and Holcomb, 1999,
388 1997).

389

390 *Interference or desensitization?*

391 We have proposed that the difference observed between the two learning blocks reflects the
392 interference of two competing memories, one associated with the feedback experienced during
393 learning and another with the feedback experienced during washout (or from a long baseline
394 block). By this view, the output of the system reflects the contribution from two memories,
395 yielding a change in behavior even if the parameters of the system (e.g., learning rate) remain
396 invariant.

397 An alternative perspective centers on the idea that the adaptation system retains a
398 memory of error history and uses this information to adjust its sensitivity to the error. For
399 example, in the Memory of Error model, the system upregulates the learning rate in response to
400 experienced or stable errors and downregulates the learning rate in response to unfamiliar or
401 variable errors (Albert et al., 2022, 2021; Coltman et al., 2019; Herzfeld et al., 2014; Yin and
402 Wei, 2020). The failure to observe savings in the implicit adaptation system, together with the
403 findings that the implicit response is the same for stable or variable errors, support the notion
404 that an increase in learning rate (i.e., savings) is likely a property of explicit processes (Avraham
405 et al., 2020; Hutter and Taylor, 2018; Wang et al., 2024a).

406 Nonetheless, attenuation upon relearning could be taken to reflect a flexible implicit
407 system, one in which the sensitivity to error decreases over learning sessions rather than
408 increases. For example, learning might become weaker due to the saturation or depletion of
409 neuroplasticity mechanisms (Hamel et al., 2022, 2021). Consistent with this hypothesis, a recent
410 study showed that attenuation was observed when there were 320 trials in the first perturbation
411 block, but not when this number was reduced to 40 trials (De La Fontaine et al., 2023).
412 However, to match the overall number of trials between the two conditions, the authors
413 extended the baseline block for participants in the short learning condition. As shown in
414 Experiments 4 and 5 above, an extended baseline block with veridical feedback attenuates
415 learning in the first block. Indeed, in De La Fontaine's study, the aftereffect of the first
416 perturbation block was smaller for the long baseline/short learning group compared to the short
417 baseline/long learning group. Thus, the absence of attenuation for the former group may be due
418 to interference in both learning blocks.

419 Nonetheless, the interference and desensitization hypotheses are not mutually
420 exclusive. Attenuation in the second learning block could be driven by a contribution from both
421 interference and desensitization (Hamel et al., 2022, 2021). However, attenuation is neither
422 observed when visual feedback is eliminated in the washout block (Experiment 2) nor during a
423 prolonged perturbation block with the same error (Avraham et al., 2021; Kim et al., 2018;
424 Morehead and Smith, 2017). Both results would appear at odds with a desensitization account,
425 at least one in which desensitization occurs as a function of the amount of experience or time
426 responding to a given perturbation. At present, we assume that interference is the primary
427 mechanism underlying attenuation upon relearning, at least in visuomotor adaptation.

428 Hadjiosif et al. (Hadjiosif et al., 2023) have suggested that the behavior during relearning
429 depends on the time-dependent decay characteristics of distinct memory components. One
430 component is a temporally volatile process that can rapidly respond to a perturbation but results

431 in a change in state that is quickly forgotten; this system is hypothesized to show heightened
432 sensitivity to experienced errors and thus drive savings. The second component is a temporally
433 stable process that exhibits slow learning but shows high retention over time; this system is
434 hypothesized to exhibit attenuation upon relearning. Our results are inconsistent with the view
435 that attenuation is restricted to a temporally stable implicit process. Given the number of target
436 locations and short inter-trial intervals in our experiments, and based on the parameters in
437 Hadjiosif et al.'s model, a temporally volatile process would still be making a significant
438 contribution to behavior in some of our conditions (e.g., in Experiment 4, the median time
439 between reaches to a given target = 1.92 s, interquartile range: [1.65 s 2.33 s], corresponding to
440 a decay of only ~5% (Hadjiosif et al., 2014)). Thus, we should have observed savings rather
441 than attenuation. We hypothesize that given the methods used in their study, the behavioral
442 changes they attribute to an implicit temporally volatile process are actually due to strategic
443 adjustments in aiming. In particular, probing implicit learning on a small subset of trials tends to
444 overestimate the implicit component (Maresch et al., 2021) as participants may fail to
445 completely dispense with an aiming strategy used in most trials (Avraham et al., 2021).

446

447 *Interference as an example of viewing adaptation from the perspective of associative learning*

448 The interference effect we observe in visuomotor adaptation is similar to a well-established
449 phenomenon in associative learning, latent inhibition (Solomon and Moore, 1975). For example,
450 in fear conditioning, pairing a neutral stimulus (conditioned stimulus, CS, e.g., a tone) with an
451 aversive electric shock (unconditioned stimulus, US) leads to a predictive fear response
452 (conditioned response, CR) to the CS. Latent inhibition refers to the finding that conditioning of a
453 CS-US pair is weaker following prolonged exposure to the CS in the absence of the US (CS-
454 alone) (Solomon and Moore, 1975). Thus, if an extended CS-alone block is used to extinguish a

455 conditioned response, reacquisition of this CR will be attenuated when the CS is again paired
456 with the US (Bouton, 1986).

457 This paradigm is structurally similar to the conditions in which we find attenuation in
458 relearning for sensorimotor adaptation: The pairing of movement with the initial feedback
459 perturbation is broken during the washout block with the introduction of discrepant feedback.
460 Furthermore, both latent inhibition and attenuation upon re-learning in adaptation exhibit context
461 specificity. An attenuated fear response was only evident in the context in which extinction was
462 experienced; when the rats were moved to a different cage between extinction and
463 reacquisition, reacquisition was not attenuated (Bouton, 2002; Bouton and Swartzentruber,
464 1989). Similarly, adaptation in Experiment 5 was attenuated in a wedge previously associated
465 with a long experience with non-perturbed feedback, but it was spared when tested in a new
466 wedge.

467 The parallels between these two types of learning may not be incidental (Calame et al.,
468 2023; Raymond et al., 1996; Villalta et al., 2015). Some forms of associative learning, like delay
469 eyeblink conditioning, share important features with implicit sensorimotor adaptation, including
470 strict constraints on the timing of the sensory feedback (Kitazawa et al., 1995; Schneiderman
471 and Gormezano, 1964; Smith et al., 1969; Wang et al., 2024b) and a strong dependency on the
472 integrity of the cerebellum (Donchin et al., 2011; Gao et al., 2016; Izawa et al., 2012; Medina et
473 al., 2000). We have recently considered the utility of a unified framework, viewing implicit
474 sensorimotor adaptation as an associative learning process (Avraham et al., 2022). In a series
475 of experiments, we demonstrated how neutral cues (tone and light) can modulate reach
476 adaptation in a manner that follows the principles of associative learning.

477 A critical issue in considering a unified framework is to examine the mechanistic overlap
478 between the components of the two processes. We have proposed that the onset of a target,
479 the typical cue for movement initiation in adaptation studies, serves as the CS, one that

480 becomes associated with the perturbed feedback (US). The repeated pairing of the CS and US
481 will increase their associated strength, resulting in an adapted movement (CR) to that target
482 even when the feedback is removed (aftereffect). When viewed in this framework, we see that
483 the target (or the movement plan associated with that target, see Avraham et al., 2022), has
484 CS-like features. For example, adaptation to nearby targets exhibits a generalization pattern
485 similar to that observed in the conditioned eyeblink response to variations in the CS (e.g., tone
486 frequency) (Krakauer et al., 2000; Siegel et al., 1968). Viewing anterograde interference in
487 adaptation as a form of latent inhibition also emphasizes that the target can be viewed as a CS.
488 Repeated movement to a target with veridical feedback will result in attenuated adaptation when
489 the target (CS) is subsequently paired with the perturbed feedback (US); this attenuation is not
490 observed for movements to distant targets.

491 One problem with the latent inhibition analogy is that we found no attenuation after a
492 long washout block in which feedback was eliminated (Experiment 2) whereas fear conditioning
493 is attenuated following a block of trials in which the CS is presented alone. Eliminating the
494 feedback in sensorimotor adaptation may not be equivalent to eliminating the US in a classical
495 conditioning study, at least when the no-feedback phase is introduced immediately after the
496 learning block. In this condition, the adaptation system may operate as if it is still in the most
497 recent context. As such, when the perturbation is re-introduced, there is no interference. By this
498 hypothesis, we would predict that using an extended block of no-feedback trials at the start of
499 an experiment, where the system is in a non-adapted, baseline state, would result in attenuation
500 in a subsequent learning block.

501 In summary, a unified framework for associative learning and sensorimotor adaptation
502 helps explain the mechanism underlying memory interference in adaptation. Prolonged
503 experience with non-perturbed feedback (e.g., during baseline or a washout block) produces a
504 strong association, perhaps in a Hebbian-like manner, between the movement plan and that

505 form of feedback (Della-Maggiore et al., 2017). From a Bayesian perspective, the participant
506 forms an inference about the causal structure of the environment, with the non-perturbed
507 feedback being linked to a specific target (the context) (Gershman et al., 2015, 2010). When
508 perturbed feedback is subsequently presented in the same context, the old association
509 interferes with the formation of a new association.

510

511 *Relevance of interference to the retention of real-world motor skills*

512 It seems paradoxical that a task as simple as implicit sensorimotor adaptation is so sensitive to
513 interference, even from veridical feedback, whereas complex skills such as bike riding or skiing
514 can be retained over many years, even without practice. However, as shown in the current
515 study, interference requires experience with discrepant feedback within a similar context. The
516 striking retention of complex motor skills may arise because they lack contextual overlap with
517 other behaviors in our motor repertoire. We preserve our ability to ride a bike because we do not
518 perform other skills sufficiently similar to produce interference.

519 The difference in complexity between simple reaching movements and skilled actions
520 may also limit how well the principles of interference identified in this study extend to more
521 complex movements. We have emphasized that interference is a feature of implicit
522 sensorimotor adaptation, a system designed to ensure that the sensorimotor system remains
523 exquisitely calibrated. While this process is surely operative in the learning and performance of
524 skilled actions, other learning processes will also be relevant to performance; it remains to be
525 seen how they are subject to interference effects. We have noted that explicit strategy use can
526 support savings. However, strategy use could also be prone to interference if a previously
527 learned strategy gets in the way of discovering a new approach (Adamson, 1952). Similarly,
528 other implicit processes essential for highly skilled behavior such as pattern identification and

529 response selection can be subject to pronounced interference effects when the task goal
530 changes (Logan, 1982; Shiffrin and Schneider, 1977).

531 In the present study, we have used a very restrictive and contrived experimental setup to
532 isolate a particular learning system and characterize one way in which the operation of this
533 system changes as a function of experience. It will be interesting to apply a similar strategy in
534 looking at other learning processes and examining more ecological tasks, with an eye on
535 identifying the conditions that support or interfere with memory consolidation.

536

537 **Methods**

538 *Ethics Statement*

539 The study was approved by the Institutional Review Board at the University of California,
540 Berkeley. All participants provided written informed consent to participate in the study and were
541 paid based on a rate of \$9.44/hr.

542

543 *Participants and experimental setup*

544 236 healthy volunteers (aged 19-38 years; 130 females, 97 males, and 9 identified as ‘other’ or
545 opted not to disclose their sex/gender identity) were tested in six experiments: 44 in each of
546 Experiments 1, 2, 3, and 4, and 60 in Experiment 5. The sample size for each experiment was
547 determined based on the effect size ($d=0.6$) observed in our previous study showing attenuation
548 of implicit adaptation upon relearning (Avraham et al., 2021), with a significance level of $\alpha=0.05$
549 and power of 0.95. The actual number allowed us to counterbalance the direction of the
550 visuomotor perturbation and, where appropriate, the target locations (detailed below).

551 We used an online platform created within the lab for conducting sensorimotor learning
552 experiments (Tsay et al., 2021a, 2020a). The platform was developed using JavaScript and
553 HTML. Participants were recruited using the crowdsourcing website Prolific (www.prolific.co)
554 and performed the experiment remotely with their personal computers. They were asked to
555 provide information concerning the size of the monitor and the device used (optical mouse or
556 trackpad), as well as their dominant hand (left, right, or ambidextrous). The program was written
557 to adjust the size of the stimuli based on a participant's monitor size. Due to an error, the data
558 from the questionnaire was not saved. However, our analysis of nearly 2,000 individuals using
559 this platform has shown that implicit visuomotor adaptation does not vary systematically
560 between response devices or handedness (Tsay et al., 2023, 2021a).

561

562 *Task*

563 At the beginning of each trial, a white circle (radius: 1% of screen height) appeared at the center
564 of the screen, indicating the start location (Fig. 1A). The participant moved a white cursor
565 (radius: 0.8% of screen height) to the start location. We refer to the body part controlling the
566 cursor — the wrist for mouse users or finger for trackpad users — as the “hand”. After the
567 cursor was maintained in the start location for 500 ms, a blue target (radius: 1% of screen
568 height) appeared at one of four or six locations (see detailed experimental protocols below)
569 positioned along a virtual circle around the start location (radial distance: 25% of screen height).

570 The participant was instructed to rapidly “reach” towards the target, attempting to slice
571 through the target with their hand. Movement time was calculated as the interval between the
572 time the center of the cursor exceeded the radius of the start location to the time at which the
573 movement amplitude reached the radial distance of the target. To encourage the participants to
574 move fast, the auditory message “too slow” was played if the movement time exceeded 300 ms.

575 After crossing the target distance, the cursor, when displayed, disappeared and the participant
576 moved back to the start location. The cursor reappeared when the hand was within 25% of the
577 radial distance from the start-to-target distance.

578 In each experiment, there were three types of feedback conditions (Fig. 1A). On no
579 feedback trials, the cursor was blanked when the hand left the start circle. On veridical feedback
580 trials, the cursor was visible and aligned with the movement direction of the hand; that is, its
581 position corresponded to the standard mapping between the mouse/trackpad and the screen
582 cursor. For the third type of trials, we used task-irrelevant clamped feedback, a visuomotor
583 perturbation that has been shown to drive implicit adaptation with minimal contamination from
584 explicit learning processes (Morehead et al., 2017). Here, the cursor moved along a fixed path,
585 displaced 15° from the target (clockwise or counterclockwise, counterbalanced across
586 participants). We opted to use a 15° clamp as a perturbation of this magnitude is within the
587 range of error sizes (~6°-60°) shown to induce the maximum rate and extent of adaptation (Kim
588 et al., 2018). The radial position of the cursor corresponded to the participant's hand position.
589 Thus, the radial position is contingent on the participant's movement, but the angular position is
590 independent of the participant's reaching direction. The participant was instructed to ignore the
591 feedback and always reach directly to the target.

592 To emphasize these instructions, three demonstration trials were performed prior to
593 each clamp block. The target location was fixed for all three trials and chosen to be at least 45°
594 from the two locations on the horizontal meridian (0° and 180°) and 45° from the nearest target
595 used for learning. In all three demonstration trials, 15° clamped feedback was provided. For the
596 first demonstration trial, the participant was instructed to "Reach straight to the left" (180°), and
597 for the second, "Reach straight to the right" (0°). Following each of these trials, a message
598 appeared to highlight that the cursor was moving away from their hand and target. For the third

599 demonstration trial, the participant was instructed to “Aim directly for the target”, emphasizing
600 again that they should ignore the cursor.

601

602 *Experimental protocol*

603 The main aim of this study was to examine the mechanisms underlying attenuation of implicit
604 sensorimotor adaptation upon relearning. The experiments described below include either one
605 or two blocks with clamped feedback to drive implicit adaptation. The learning blocks were
606 surrounded by blocks with various types of feedback depending on the design of each
607 experiment. Throughout the paper, we use the following convention to describe the
608 experimental protocols. -C refers to a learning block with clamped feedback. The minus (-) sign
609 indicates a perturbation direction that is opposite from the expected direction of adaptation. C
610 (without the minus sign) refers to blocks using a clamp that is rotated in the opposite direction of
611 the clamp used during the learning blocks. V refers to blocks with veridical feedback. N refers to
612 blocks with no feedback. The non-learning blocks, which constitute the main manipulations
613 across our experiments, are highlighted in bold fonts and are separated from the learning blocks
614 using the | sign.

615 Experiment 1: Readaptation following standard washout (-C|CV|-C design)

616 Experiment 1 was designed to provide a replication of our previous finding that implicit
617 adaptation is attenuated upon relearning (Avraham et al., 2021). The main protocol included two
618 learning blocks separated by a washout block (-C|CV|-C). The experimental session consisted
619 of 300 movement cycles, each involving one movement to each of four target locations: 45°,
620 135°, 225°, 335° (1200 movements in total). The four targets appeared in a pseudorandom and
621 predetermined order within a cycle. The session was composed of the following blocks (Fig.

622 1B): No Feedback (5 cycles), Veridical Feedback (5 cycles), Learning 1 (80 cycles), Aftereffect
623 1 (10 cycles), Washout (110 cycles), Learning 2 (80 cycles) and Aftereffect 2 (10 cycles).

624 The two initial blocks (No Feedback and Veridical Feedback) were included to familiarize
625 the participants with the experimental setup. For these trials, participants were instructed to
626 move their hand directly to the target. By providing veridical feedback in the second block, we
627 expected to minimize idiosyncratic reaching biases. The two learning blocks are the blocks in
628 which we expected to observe implicit adaptation. The aftereffect blocks provided an additional
629 assessment of adaptation. These occurred immediately after the learning blocks, and visual
630 feedback was absent in these trials. Just before the start of the aftereffect block, an instruction
631 screen informed the participant that the cursor would no longer be visible and reminded them
632 that their task was to move directly to the target. The participant pressed a key to start the
633 aftereffect block. While some forgetting might occur during this break, we anticipate that the
634 delay was short. Indeed, the reach angle during the first cycle of the aftereffect block closely
635 matched the reach angle during the last 10 cycles of the learning block ([mean Aftereffect (1st
636 cycle) / Late learning, 95% confidence interval, CI], Learning 1: 0.92, [0.81 1.04], Learning 2:
637 0.99, [0.85 1.14]).

638 The washout block was used to bring behavior back to baseline. Typically in studies of
639 relearning in sensorimotor adaptation, washout is administered by removing the perturbation
640 (e.g., the rotation of the cursor) and providing veridical feedback (Albert et al., 2022; Herzfeld et
641 al., 2014; Huang et al., 2011; Krakauer et al., 2005; Morehead et al., 2015; Yin and Wei, 2020;
642 Zarahn et al., 2008). However, assuming adaptation has occurred, the introduction of veridical
643 feedback after adaptation results in a relatively large discrepancy between the expected and
644 observed feedback. We were concerned that this would make participants aware of the change
645 in behavior induced by the clamp, and that this might alter their behavior in the second learning
646 block (e.g., invoke a strategy to offset the anticipated effects of adaptation). To minimize

647 awareness of adaptation, the washout block consisted of two phases (Fig. 1B) (Avraham et al.,
648 2021). In the first phase, we reversed the direction of the clamp. The participant was informed
649 that they would again not have control over the movement direction of the feedback, and they
650 were reminded to ignore the feedback and aim directly for the target. The reversed clamp will
651 reverse adaptation, driving the direction of the hand back towards the target. When the median
652 reach direction was within 5° of the targets for five consecutive cycles, the second phase was
653 implemented with the feedback now veridical.

654 Demonstration trials were provided at the start of each phase of the washout block, three
655 for the reversed clamp and three for veridical feedback. The demonstration trials were similar to
656 those presented before the learning blocks (same target location and same instructions for
657 where to reach). Note that the demonstration trials for the phase with veridical feedback
658 appeared when the participant's reaches were relatively close to the target. As such, we
659 expected that participants would be unaware of any residual adaptation at the start of this
660 phase. We did not assess participants' awareness about their change in behavior during
661 learning. However, when surveyed in a previous study that used the same procedure, none of
662 the participants reported awareness of any learning-related changes in their behavior (Avraham
663 et al., 2021).

664 We opted to keep the total number of washout cycles fixed. Thus, the number of cycles
665 in each phase of the washout block was determined on an individual basis using the
666 performance criterion described above. All participants experienced at least 70 cycles (mean ±
667 standard deviation, 91.3±13.4) of veridical feedback before the second clamp block, ensuring
668 they had sufficient exposure to unperturbed feedback before the onset of the second learning
669 block.

670 Experiment 2: Readaptation following no feedback washout (-C|N|-C design)

671 Experiment 2 was designed to test if the attenuation of implicit adaptation upon relearning is due
672 to interference from the feedback experienced during washout. To this end, we tested a
673 condition in which feedback was withheld during the entire washout block (Fig. 2A). The
674 protocol was similar to Experiment 1 with one change: We eliminated the feedback in the 110-
675 cycle washout block (-C|N|-C design). As such, the washout block was identical to the preceding
676 aftereffect block.

677 Experiment 3: Readaptation following gradual rotation washout (-C|R_GV|-C design)

678 Experiment 3 was designed to test if experience with salient, opposite-signed errors at the
679 beginning of the washout block (e.g., the reversed-clamped feedback in Experiment 1) is
680 required to attenuate adaptation upon relearning. The protocol was similar to that used in
681 Experiment 1 with the difference being the procedure used in the washout block. To minimize
682 exposure to large opposite errors, we used rotated feedback that was contingent on the
683 movement of the hand and tailored on an individual basis. For each participant, we calculated
684 the mean reach angle during the first aftereffect block and, for the first cycle of the washout
685 block, rotated the cursor from the actual hand position by that angle multiplied by -1 (Fig. 3A, -
686 C|R_GV|-C design). In this way, the rotated visual feedback should counteract the effects of
687 adaptation, with the net effect that the cursor would cross relatively close to the target. On each
688 successive cycle, the size of the rotation was decreased by 1° until it reached zero (veridical
689 feedback). For the remainder of the washout block, the feedback was veridical.

690 At the beginning of the washout block, participants were told that the cursor would now
691 be aligned with their hand position. We added three demonstration trials to reinforce these
692 instructions. These trials were similar to the demonstration trials used to illustrate the clamped
693 feedback (same target location and instructions of aiming direction). Since the target location
694 used for the demonstration trials (270°) was 45° from the nearest target locations used for
695 adaptation (225° and 315°), we expected a generalization of ~25% adaptation for reaches to the

696 demonstration locations (Morehead et al., 2017). Thus, the rotation size during these
697 demonstration trials was set to be 25% of the magnitude of the participant's aftereffect. We
698 assumed this would give the impression that the cursor was aligned with the participant's
699 movement.

700 **Experiment 4: Adaptation following extended veridical feedback ($V_{85}|C$)**

701 Experiment 4 was designed to test if extended exposure to veridical feedback was sufficient to
702 produce attenuation of subsequent adaptation. The experimental session consisted of 150
703 cycles, each consisting of one movement to each of four targets: 30°, 60°, 210°, 240° (Fig. 4A).
704 The four targets appeared in a pseudorandom and predetermined order within a cycle. Adjacent
705 targets were paired [(30°, 60°) and (210°, 240°)] to define a wedge.

706 For one wedge, we used a -C|CV|-C design, consisting of No Feedback (5 cycles),
707 Veridical Feedback (5 cycles), Learning 1 (40 cycles), Aftereffect 1 (10 cycles), Washout (40
708 cycles), Learning 2 (40 cycles), and Aftereffect 2 (10 cycles). As in Experiment 1, the washout
709 block consisted of a reversed clamp phase and a veridical feedback phase, with the transition
710 between the two phases adjusted on an individual basis (see above). For the second wedge, we
711 used a $V_{85}|C$ design, consisting of No Feedback (5 cycles), Veridical Feedback (85 cycles, with
712 an additional 10 cycle block of No Feedback inserted between cycles 50 and 61), Learning (40
713 cycles), and Aftereffect (10 cycles). Before each learning block, the participant was provided
714 with a full description of the nature of the feedback for each wedge. In addition, six
715 demonstration trials (three for each wedge) were provided to emphasize the instructions. The
716 association between the wedge location and protocol was counterbalanced across participants.

717 **Experiment 5: Adaptation following varying experiences with veridical feedback at distinct**
718 **contexts ($V_5|C$ / $V_{45}|C$ / $V_{85}|C$ design)**

719 Experiment 5 examined if the interference effect from veridical feedback is context specific. The
720 target could appear at one of six locations: 10°, 40°, 130°, 160°, 250°, 280° (Fig. 5A). Pairs of
721 adjacent targets defined three wedges [(10°, 40°), (130°, 160°) and (250°, 280°)], and the
722 number of veridical feedback cycles prior to adaptation varied across the three wedges. The
723 session started with a 5-cycle No Feedback block in which participants moved to each of the six
724 targets, with the locations selected in a random order (within a cycle). This was followed by a
725 Veridical Feedback block (85 cycles). However, the number of wedges included in each cycle
726 changed over the course of the block. In the first phase (40 cycles), the target only appeared in
727 the two locations that defined one wedge; in the second phase (40 cycles), a second wedge
728 was added; and in the third phase (5 cycles), the remaining wedge was included. In this
729 manner, each wedge (counterbalanced across participants) was associated with a different
730 number of veridical feedback trials prior to learning: 5 (V_5 -C), 45 (V_{45} -C) or 85 (V_{85} -C) cycles.
731 This was followed by a Learning block (40 cycles) and an Aftereffect block (10 cycles); within
732 each of these, all six targets were included in each cycle.

733

734 *Data analysis*

735 The kinematic data recorded from the mouse/trackpad were temporarily stored on the Google
736 Firebase database and downloaded for offline analyses using custom-written MATLAB codes.
737 The primary dependent variable was the direction of hand movement (reach angle). Reach
738 angle was defined by two lines, one from the start position to the target and the other from the
739 start position to the hand position at the moment it crossed the radial distance of the target. For
740 participants who experienced a counterclockwise clamp during the learning blocks, the sign of
741 the reach angle was flipped. In this manner, a positive reach angle indicates movement in the
742 opposite direction of the perturbed feedback, the expected change due to adaptation. The reach

743 angle for each movement cycle was calculated by averaging the reach angle of all reaches
744 within a cycle, one to each of the different target locations.

745 We excluded trials in which the reach angle deviated from the target location by more
746 than 100° and trials in which the absolute trial-to-trial change in reach angle was larger than 20°
747 (Avraham et al., 2021). Based on these criteria, a total of 1.97% of all trials were excluded.

748 For Experiment 3, we plotted the distribution of errors participants experienced during
749 the non-zero rotation trials of the washout block (Fig. 3B). To evaluate this distribution with
750 respect to an error distribution for veridical feedback (Fig. S2), we used data from another group
751 of participants (N=44). This group experienced an extended, 195-cycle block with veridical
752 feedback. To plot the distribution, we used the data from cycles 100-116, matching the phase of
753 the experiment and the mean number of trials used for calculating the distribution in Experiment
754 3.

755

756 *Statistical analysis*

757 Two statistical approaches were used to analyze the changes in reach angle that occurred in
758 response to the clamped feedback. For the first approach, we used a nonparametric
759 permutation test to identify clusters of cycles in which the reach angle differed between
760 conditions (Avraham et al., 2021; Labruna et al., 2019; Maris and Oostenveld, 2007). For
761 example, to examine within-participant changes in adaptation between the first and the second
762 learning in Experiment 1 (Fig. 1C), a two-tailed paired-sample *t* test was performed for each
763 cycle within the learning and aftereffect blocks.

764 We defined consecutive cycles in which the difference was significant ($p < 0.05$) as a
765 'cluster' and calculated for each cluster the sum of the *t*-values that were obtained for the cycles
766 in that cluster (referred to as a *t*-sum statistic). A null distribution of the *t*-sum statistic was

767 constructed by performing 10,000 random permutations with the data: For each permutation,
768 the data for a given participant was randomly assigned to “block 1” or “block 2”. For each
769 permuted data set, we performed the same cluster-identification procedure as was done with
770 the actual data and calculated the t-sum statistic for each cluster. In cases where several
771 clusters were found for a given null set permutation, we recorded the t-sum statistic of the
772 cluster with the largest t-sum value. Thus, the generated null distribution is composed of the
773 maximal t-sum values achieved by chance, a method that controls for the multiple comparisons
774 involved in this analysis (Maris and Oostenveld, 2007). Each of the clusters identified in the non-
775 permuted data were considered statistically significant if its t-sum was larger than 95% of the t-
776 sums in the null distribution, corresponding to a *p*-value of 0.05.

777 The same analysis was used to assess within-participants changes in reach angle
778 between two learning and aftereffect blocks in Experiments 1, 2, 3, and 4. For Experiment 4, we
779 did this procedure three times, for the following comparisons: Learning 2 in the -C|CV|-C
780 location vs Learning 2 in the V₈₅-C location, Learning 1 vs Learning 2 in the -C|CV|-C location,
781 and Learning 1 in the -C|CV|-C location vs Learning 2 in the V₈₅-C location. Therefore, we
782 increased the threshold to identify significant clusters against the null distribution to 98.3%,
783 corresponding to *p*-value of 0.05/3=0.017.

784 In Experiment 5, we had three conditions that varied in the number of cycles of veridical
785 feedback before learning (85, 45 and 5 cycles). We hypothesized that the extent of adaptation
786 would decrease with the increased experience with veridical feedback. Therefore, we used a
787 linear regression analysis, with the response variable (*y*) being the mean cycle reach angle and
788 the predictor variable (*X*) being the number of veridical feedback cycles. We included a constant
789 intercept. We extracted the slope of the regression line for each cycle, and submitted that to the
790 non-parametric, cluster-based permutation analysis. Thus, significant clusters in Figure 5A
791 represent clusters of cycles in which the slope of the regression is significantly different than

792 zero (and negative, representing a decrease in adaptation with increasing experience with
793 veridical feedback) against a null distribution.

794 The second approach focused on the aftereffect measure of adaptation. This was
795 defined as the mean reach angle over all ten cycles of the aftereffect block. To examine
796 changes in adaptation between the two blocks in Experiments 1, 2, and 3, we used two-tailed
797 paired-sample *t* tests. For the within-participant comparisons of the aftereffect across conditions
798 in Experiments 4, we used a one-way repeated measures ANOVA. The sphericity assumption
799 was violated in Experiment 4, and thus, the *F*-test degrees of freedom was adjusted using the
800 Greenhouse–Geisser correction. For Experiment 5, we used a linear mixed-effect model to fit
801 the aftereffect data, including fixed-effect slope and intercept for the number of veridical cycles
802 before learning (4, 45, and 85) and random-effect slope and intercept for the individual
803 participants. For all of the experiments, the statistical significance threshold was set at the
804 $p < 0.05$. p_B denotes the Bonferroni corrected p-value. In addition, we report the Bayes factor
805 BF_{10} , the ratio of the likelihood of the alternative hypothesis (H_1) over the null hypothesis (H_0)
806 (Kass and Raftery, 1995). For *t*-tests, we report the Cohen's *d* effect size (Cohen, 2013), and for
807 the repeated-measures ANOVAs, we report effect sizes using partial eta-squared (η_p^2). We
808 followed the assumption of normality based on the central limit theorem as the sample size for
809 all experiments was larger than $N=30$.

810

811 *Data and code availability*

812 All raw data files and codes for data analysis are available from the GitHub repository:
813 <https://github.com/guyavr/InterferenceRelearningMotorAdaptation.git>

814

815 **Acknowledgments**

816 We thank Maya Malaviya for her assistance with data collection. This work was supported by
817 grants NS116883, DC077091 from the National Institutes of Health (NIH).

818

819 **Competing interests**

820 RBI is a co-founder with equity in Magnetic Tides, Inc.

821 **References**

- 822 Adamson RE. 1952. Functional fixedness as related to problem solving: a repetition of three
823 experiments. *Journal of Experimental Psychology* **44**:288–291. doi:10.1037/h0062487
- 824 Albert ST, Jang J, Modchalingam S, 't Hart BM, Henriques D, Lerner G, Della-Maggiore V, Haith AM,
825 Krakauer JW, Shadmehr R. 2022. Competition between parallel sensorimotor learning systems.
826 *eLife* **11**:e65361. doi:10.7554/eLife.65361
- 827 Albert ST, Jang J, Sheahan HR, Teunissen L, Vandevenne K, Herzfeld DJ, Shadmehr R. 2021. An implicit
828 memory of errors limits human sensorimotor adaptation. *Nature Human Behaviour* 1–15.
829 doi:10.1038/s41562-020-01036-x
- 830 Avraham G, Keizman M, Shmuelof L. 2020. Environmental consistency modulation of error sensitivity
831 during motor adaptation is explicitly controlled. *Journal of Neurophysiology* **123**:57–69.
832 doi:10.1152/jn.00080.2019
- 833 Avraham G, Morehead JR, Kim HE, Ivry RB. 2021. Reexposure to a sensorimotor perturbation produces
834 opposite effects on explicit and implicit learning processes. *PLOS Biology* **19**:e3001147.
835 doi:10.1371/journal.pbio.3001147
- 836 Avraham G, Taylor JA, Breska A, Ivry RB, McDougle SD. 2022. Contextual effects in sensorimotor
837 adaptation adhere to associative learning rules. *eLife* **11**:e75801. doi:10.7554/eLife.75801
- 838 Bock O, Schneider S, Bloomberg J. 2001. Conditions for interference versus facilitation during sequential
839 sensorimotor adaptation. *Exp Brain Res* **138**:359–365. doi:10.1007/s002210100704
- 840 Bond KM, Taylor JA. 2015. Flexible explicit but rigid implicit learning in a visuomotor adaptation task.
841 *Journal of Neurophysiology* **113**:3836–3849. doi:10.1152/jn.00009.2015
- 842 Bouton ME. 2002. Context, ambiguity, and unlearning: sources of relapse after behavioral extinction.
843 *Biological Psychiatry* **52**:976–986. doi:10.1016/S0006-3223(02)01546-9

- 844 Bouton ME. 1986. Slow reacquisition following the extinction of conditioned suppression. *Learning and*
845 *Motivation* **17**:1–15. doi:10.1016/0023-9690(86)90017-2
- 846 Bouton ME, Swartzentruber D. 1989. Slow reacquisition following extinction: Context, encoding, and
847 retrieval mechanisms. *Journal of Experimental Psychology: Animal Behavior Processes* **15**:43–53.
848 doi:10.1037/0097-7403.15.1.43
- 849 Brashers-Krug T, Shadmehr R, Bizzi E. 1996. Consolidation in human motor memory. *Nature* **382**:252–
850 255. doi:10.1038/382252a0
- 851 Caithness G, Osu R, Bays P, Chase H, Klassen J, Kawato M, Wolpert DM, Flanagan JR. 2004. Failure to
852 consolidate the Consolidation Theory of Learning for Sensorimotor Adaptation Tasks. *J Neurosci*
853 **24**:8662–8671. doi:10.1523/JNEUROSCI.2214-04.2004
- 854 Calame DJ, Becker MI, Person AL. 2023. Cerebellar associative learning underlies skilled reach
855 adaptation. *Nat Neurosci* **26**:1068–1079. doi:10.1038/s41593-023-01347-y
- 856 Christou AI, Miall RC, McNab F, Galea JM. 2016. Individual differences in explicit and implicit visuomotor
857 learning and working memory capacity. *Sci Rep* **6**:36633. doi:10.1038/srep36633
- 858 Cohen J. 2013. Statistical Power Analysis for the Behavioral Sciences. Academic Press.
- 859 Coltman SK, Cashaback JGA, Gribble PL. 2019. Both fast and slow learning processes contribute to
860 savings following sensorimotor adaptation. *Journal of Neurophysiology* **121**:1575–1583.
861 doi:10.1152/jn.00794.2018
- 862 Criscimagna-Hemminger SE, Shadmehr R. 2008. Consolidation Patterns of Human Motor Memory. *J*
863 *Neurosci* **28**:9610–9618. doi:10.1523/JNEUROSCI.3071-08.2008
- 864 De La Fontaine E, Hamel R, Lepage JF, Bernier PM. 2023. The influence of learning history on
865 anterograde interference. *Neurobiology of Learning and Memory* **206**:107866.
866 doi:10.1016/j.nlm.2023.107866

- 867 Della-Maggiore V, Villalta JI, Kovacevic N, McIntosh AR. 2017. Functional Evidence for Memory
868 Stabilization in Sensorimotor Adaptation: A 24-h Resting-State fMRI Study. *Cerebral Cortex*
869 **27**:1748–1757. doi:10.1093/cercor/bhv289
- 870 Donchin O, Rabe K, Diedrichsen J, Lally N, Schoch B, Gizewski ER, Timmann D. 2011. Cerebellar regions
871 involved in adaptation to force field and visuomotor perturbation. *Journal of Neurophysiology*
872 **107**:134–147. doi:10.1152/jn.00007.2011
- 873 Doyon J, Korman M, Morin A, Dostie V, Tahar AH, Benali H, Karni A, Ungerleider LG, Carrier J. 2009.
874 Contribution of night and day sleep vs. simple passage of time to the consolidation of motor
875 sequence and visuomotor adaptation learning. *Exp Brain Res* **195**:15–26. doi:10.1007/s00221-
876 009-1748-y
- 877 Ebbinghaus H. 1913. Memory (ha ruger & ce bussenius, trans.). New York: Teachers College(*Original
878 work published 1885*) **39**.
- 879 Gao Z, Proietti-Onori M, Lin Z, ten Brinke MM, Boele H-J, Potters J-W, Ruigrok TJH, Hoebeek FE,
880 De Zeeuw CI. 2016. Excitatory Cerebellar Nucleocortical Circuit Provides Internal Amplification
881 during Associative Conditioning. *Neuron* **89**:645–657. doi:10.1016/j.neuron.2016.01.008
- 882 Gershman SJ, Blei DM, Niv Y. 2010. Context, learning, and extinction. *Psychological Review* **117**:197–209.
883 doi:10.1037/a0017808
- 884 Gershman SJ, Norman KA, Niv Y. 2015. Discovering latent causes in reinforcement learning. *Current
885 Opinion in Behavioral Sciences, Neuroeconomics* **5**:43–50. doi:10.1016/j.cobeha.2015.07.007
- 886 Goedert KM, Willingham DB. 2002. Patterns of Interference in Sequence Learning and Prism Adaptation
887 Inconsistent With the Consolidation Hypothesis. *Learn Mem* **9**:279–292. doi:10.1101/lm.50102
- 888 Hadjiosif AM, Criscimagna-Hemminger SE, Gibo TL, Okamura AM, Shadmehr R, Bastian AJ, Smith MA.
889 2014. Cerebellar damage reduces the stability of motor memories. *Proceeding of the
890 translational and computational motor control.*

- 891 Hadjiosif AM, Morehead JR, Smith MA. 2023. A double dissociation between savings and long-term
892 memory in motor learning. *PLOS Biology* **21**:e3001799. doi:10.1371/journal.pbio.3001799
- 893 Haith AM, Huberdeau DM, Krakauer JW. 2015. The Influence of Movement Preparation Time on the
894 Expression of Visuomotor Learning and Savings. *J Neurosci* **35**:5109–5117.
895 doi:10.1523/JNEUROSCI.3869-14.2015
- 896 Hamel R, Dallaire-Jean L, De La Fontaine É, Lepage JF, Bernier PM. 2021. Learning the same motor task
897 twice impairs its retention in a time- and dose-dependent manner. *Proceedings of the Royal
898 Society B: Biological Sciences* **288**:20202556. doi:10.1098/rspb.2020.2556
- 899 Hamel R, Lepage J-F, Bernier P-M. 2022. Anterograde interference emerges along a gradient as a
900 function of task similarity: A behavioural study. *European Journal of Neuroscience* **55**:49–66.
901 doi:10.1111/ejn.15561
- 902 Heald JB, Lengyel M, Wolpert DM. 2021. Contextual inference underlies the learning of sensorimotor
903 repertoires. *Nature* 1–5. doi:10.1038/s41586-021-04129-3
- 904 Herzfeld DJ, Vaswani PA, Marko M, Shadmehr R. 2014. A memory of errors in sensorimotor learning.
905 *Science* 1253138. doi:10.1126/science.1253138
- 906 Hinder MR, Walk L, Woolley DG, Riek S, Carson RG. 2007. The interference effects of non-rotated versus
907 counter-rotated trials in visuomotor adaptation. *Exp Brain Res* **180**:629–640.
908 doi:10.1007/s00221-007-0888-1
- 909 Huang VS, Haith A, Mazzoni P, Krakauer JW. 2011. Rethinking Motor Learning and Savings in Adaptation
910 Paradigms: Model-Free Memory for Successful Actions Combines with Internal Models. *Neuron*
911 **70**:787–801. doi:10.1016/j.neuron.2011.04.012
- 912 Huberdeau DM, Krakauer JW, Haith AM. 2019. Practice induces a qualitative change in the memory
913 representation for visuomotor learning. *Journal of Neurophysiology* **122**:1050–1059.
914 doi:10.1152/jn.00830.2018

- 915 Hutter SA, Taylor JA. 2018. Relative sensitivity of explicit reaiming and implicit motor adaptation. *Journal
916 of Neurophysiology* **120**:2640–2648. doi:10.1152/jn.00283.2018
- 917 Izawa J, Criscimagna-Hemminger SE, Shadmehr R. 2012. Cerebellar Contributions to Reach Adaptation
918 and Learning Sensory Consequences of Action. *J Neurosci* **32**:4230–4239.
919 doi:10.1523/JNEUROSCI.6353-11.2012
- 920 Kass RE, Raftery AE. 1995. Bayes Factors. *Journal of the American Statistical Association* **90**:773–795.
921 doi:10.1080/01621459.1995.10476572
- 922 Kim HE, Avraham G, Ivry RB. 2021. The Psychology of Reaching: Action Selection, Movement
923 Implementation, and Sensorimotor Learning. *Annual Review of Psychology* **72**:61–95.
924 doi:10.1146/annurev-psych-010419-051053
- 925 Kim HE, Morehead JR, Parvin DE, Moazzezi R, Ivry RB. 2018. Invariant errors reveal limitations in motor
926 correction rather than constraints on error sensitivity. *Communications Biology* **1**:19.
927 doi:10.1038/s42003-018-0021-y
- 928 Kitazawa S, Kohno T, Uka T. 1995. Effects of delayed visual information on the rate and amount of prism
929 adaptation in the human. *J Neurosci* **15**:7644–7652. doi:10.1523/JNEUROSCI.15-11-07644.1995
- 930 Kojima Y, Iwamoto Y, Yoshida K. 2004. Memory of Learning Facilitates Saccadic Adaptation in the
931 Monkey. *J Neurosci* **24**:7531–7539. doi:10.1523/JNEUROSCI.1741-04.2004
- 932 Krakauer JW. 2009. Motor Learning and Consolidation: The Case of Visuomotor Rotation In: Sternad D,
933 editor. *Progress in Motor Control: A Multidisciplinary Perspective, Advances in Experimental
934 Medicine and Biology*. Boston, MA: Springer US. pp. 405–421. doi:10.1007/978-0-387-77064-
935 2_21
- 936 Krakauer JW, Ghez C, Ghilardi MF. 2005. Adaptation to Visuomotor Transformations: Consolidation,
937 Interference, and Forgetting. *J Neurosci* **25**:473–478. doi:10.1523/JNEUROSCI.4218-04.2005

- 938 Krakauer JW, Ghilardi M-F, Ghez C. 1999. Independent learning of internal models for kinematic and
939 dynamic control of reaching. *Nat Neurosci* **2**:1026–1031. doi:10.1038/14826
- 940 Krakauer JW, Pine ZM, Ghilardi M-F, Ghez C. 2000. Learning of Visuomotor Transformations for Vectorial
941 Planning of Reaching Trajectories. *J Neurosci* **20**:8916–8924. doi:10.1523/JNEUROSCI.20-23-
942 08916.2000
- 943 Labruna L, Stark-Inbar A, Breska A, Dabit M, Vanderschelden B, Nitsche MA, Ivry RB. 2019. Individual
944 differences in TMS sensitivity influence the efficacy of tDCS in facilitating sensorimotor
945 adaptation. *Brain Stimulation* **12**:992–1000. doi:10.1016/j.brs.2019.03.008
- 946 Leow L-A, Loftus AM, Hammond GR. 2012. Impaired savings despite intact initial learning of motor
947 adaptation in Parkinson’s disease. *Exp Brain Res* **218**:295–304. doi:10.1007/s00221-012-3060-5
- 948 Leow L-A, Marinovic W, Rugy A de, Carroll TJ. 2020. Task Errors Drive Memories That Improve
949 Sensorimotor Adaptation. *J Neurosci* **40**:3075–3088. doi:10.1523/JNEUROSCI.1506-19.2020
- 950 Logan GD. 1982. On the ability to inhibit complex movements: A stop-signal study of typewriting. *Journal
951 of Experimental Psychology: Human Perception and Performance* **8**:778–792. doi:10.1037/0096-
952 1523.8.6.778
- 953 Maresch J, Werner S, Donchin O. 2021. Methods matter: Your measures of explicit and implicit
954 processes in visuomotor adaptation affect your results. *European Journal of Neuroscience*
955 **53**:504–518. doi:10.1111/ejn.14945
- 956 Maris E, Oostenveld R. 2007. Nonparametric statistical testing of EEG- and MEG-data. *Journal of
957 Neuroscience Methods* **164**:177–190. doi:10.1016/j.jneumeth.2007.03.024
- 958 Mawase F, Shmuelof L, Bar-Haim S, Karniel A. 2014. Savings in locomotor adaptation explained by
959 changes in learning parameters following initial adaptation. *Journal of Neurophysiology*
960 **111**:1444–1454. doi:10.1152/jn.00734.2013

- 961 McDougle SD, Bond KM, Taylor JA. 2017. Implications of plan-based generalization in sensorimotor
962 adaptation. *Journal of Neurophysiology* **118**:383–393. doi:10.1152/jn.00974.2016
- 963 Medina JF, Garcia KS, Mauk MD. 2001. A Mechanism for Savings in the Cerebellum. *J Neurosci* **21**:4081–
964 4089. doi:10.1523/JNEUROSCI.21-11-04081.2001
- 965 Medina JF, Nores WL, Ohyama T, Mauk MD. 2000. Mechanisms of cerebellar learning suggested by
966 eyelid conditioning. *Current Opinion in Neurobiology* **10**:717–724. doi:10.1016/S0959-
967 4388(00)00154-9
- 968 Miall RC, Jenkinson N, Kulkarni K. 2004. Adaptation to rotated visual feedback: a re-examination of
969 motor interference. *Exp Brain Res* **154**:201–210. doi:10.1007/s00221-003-1630-2
- 970 Milner B. 1962. Physiologie de l’Hippocampe: Colloque International, No. 107, Editions du Centre
971 National de la Recherche Scientifique, Paris, 1962. 512 pp. 58NF. Pergamon.
- 972 Modchalingam S, Ciccone M, D’Amario S, ’t Hart BM, Henriques DYP. 2023. Adapting to visuomotor
973 rotations in stepped increments increases implicit motor learning. *Sci Rep* **13**:5022.
974 doi:10.1038/s41598-023-32068-8
- 975 Morehead JR, Qasim SE, Crossley MJ, Ivry R. 2015. Savings upon Re-Aiming in Visuomotor Adaptation. *J
976 Neurosci* **35**:14386–14396. doi:10.1523/JNEUROSCI.1046-15.2015
- 977 Morehead JR, Smith M. 2017. The magnitude of implicit sensorimotor adaptation is limited by
978 continuous forgettingAbstract. *Advances in Motor Learning & Motor Control*, Washington DC.
- 979 Morehead JR, Taylor JA, Parvin DE, Ivry RB. 2017. Characteristics of Implicit Sensorimotor Adaptation
980 Revealed by Task-irrelevant Clamped Feedback. *Journal of Cognitive Neuroscience* **29**:1061–
981 1074. doi:10.1162/jocn_a_01108
- 982 Nguyen-Vu TB, Zhao GQ, Lahiri S, Kimpo RR, Lee H, Ganguli S, Shatz CJ, Raymond JL. 2017. A saturation
983 hypothesis to explain both enhanced and impaired learning with enhanced plasticity. *eLife*
984 **6**:e20147. doi:10.7554/eLife.20147

- 985 Raymond JL, Lisberger SG, Mauk MD. 1996. The Cerebellum: A Neuronal Learning Machine? *Science*
986 **272**:1126–1131. doi:10.1126/science.272.5265.1126
- 987 Schneiderman N, Gormezano I. 1964. Conditioning of the nictitating membrane of the rabbit as a
988 function of CS-US interval. *Journal of Comparative and Physiological Psychology* **57**:188–195.
989 doi:10.1037/h0043419
- 990 Shadmehr R, Holcomb HH. 1999. Inhibitory control of competing motor memories. *Exp Brain Res*
991 **126**:235–251. doi:10.1007/s002210050733
- 992 Shadmehr R, Holcomb HH. 1997. Neural Correlates of Motor Memory Consolidation. *Science* **277**:821–
993 825. doi:10.1126/science.277.5327.821
- 994 Shiffrin RM, Schneider W. 1977. Controlled and automatic human information processing: II. Perceptual
995 learning, automatic attending and a general theory. *Psychological Review* **84**:127–190.
996 doi:10.1037/0033-295X.84.2.127
- 997 Siegel S, Hearst E, George N. 1968. Generalization gradients obtained from individual subjects following
998 classical conditioning. *Journal of Experimental Psychology* **78**:171–174. doi:10.1037/h0026178
- 999 Sing GC, Smith MA. 2010. Reduction in Learning Rates Associated with Anterograde Interference Results
1000 from Interactions between Different Timescales in Motor Adaptation. *PLOS Computational
1001 Biology* **6**:e1000893. doi:10.1371/journal.pcbi.1000893
- 1002 Smith MC, Coleman SR, Gormezano I. 1969. Classical conditioning of the rabbit's nictitating membrane
1003 response at backward, simultaneous, and forward CS-US intervals. *Journal of Comparative and
1004 Physiological Psychology* **69**:226–231. doi:10.1037/h0028212
- 1005 Solomon PR, Moore JW. 1975. Latent inhibition and stimulus generalization of the classically
1006 conditioned nictitating membrane response in rabbits (*Oryctolagus cuniculus*) following
1007 hippocampal ablation. *Journal of Comparative and Physiological Psychology* **89**:1192–1203.
1008 doi:10.1037/h0077183

- 1009 Stark-Inbar A, Raza M, Taylor JA, Ivry RB. 2016. Individual differences in implicit motor learning: task
1010 specificity in sensorimotor adaptation and sequence learning. *Journal of Neurophysiology*
1011 **117**:412–428. doi:[10.1152/jn.01141.2015](https://doi.org/10.1152/jn.01141.2015)
- 1012 Taylor JA, Krakauer JW, Ivry RB. 2014. Explicit and Implicit Contributions to Learning in a Sensorimotor
1013 Adaptation Task. *J Neurosci* **34**:3023–3032. doi:[10.1523/JNEUROSCI.3619-13.2014](https://doi.org/10.1523/JNEUROSCI.3619-13.2014)
- 1014 Tsay JS, Asmerian H, Germine LT, Wilmer J, Ivry RB, Nakayama K. 2023. Predictors of sensorimotor
1015 adaption: insights from over 100,000 reaches. doi:[10.1101/2023.01.18.524634](https://doi.org/10.1101/2023.01.18.524634)
- 1016 Tsay JS, Ivry RB, Lee A, Avraham G. 2021a. Moving outside the lab: The viability of conducting
1017 sensorimotor learning studies online. *NBDT* **5**:1–22. doi:[10.51628/001c.26985](https://doi.org/10.51628/001c.26985)
- 1018 Tsay JS, Kim HE, Parvin DE, Stover AR, Ivry RB. 2021b. Individual differences in proprioception predict the
1019 extent of implicit sensorimotor adaptation. *Journal of Neurophysiology* **125**:1307–1321.
1020 doi:[10.1152/jn.00585.2020](https://doi.org/10.1152/jn.00585.2020)
- 1021 Tsay JS, Lee AS, Avraham G, Parvin DE, Ho J, Boggess M, Woo R, Nakayama K, Ivry RB. 2020a. OnPoint: A
1022 package for online experiments in motor control and motor learning. PsyArXiv.
1023 doi:[10.31234/osf.io/hwmpy](https://doi.org/10.31234/osf.io/hwmpy)
- 1024 Tsay JS, Parvin DE, Ivry RB. 2020b. Continuous reports of sensed hand position during sensorimotor
1025 adaptation. *Journal of Neurophysiology* **124**:1122–1130. doi:[10.1152/jn.00242.2020](https://doi.org/10.1152/jn.00242.2020)
- 1026 Underwood BJ. 1957. Interference and forgetting. *Psychological Review* **64**:49–60.
1027 doi:[10.1037/h0044616](https://doi.org/10.1037/h0044616)
- 1028 Villalta JI, Landi SM, Fló A, Della-Maggiore V. 2015. Extinction Interferes with the Retrieval of
1029 Visuomotor Memories Through a Mechanism Involving the Sensorimotor Cortex. *Cereb Cortex*
1030 **25**:1535–1543. doi:[10.1093/cercor/bht346](https://doi.org/10.1093/cercor/bht346)

- 1031 Walker MP, Brakefield T, Morgan A, Hobson JA, Stickgold R. 2002. Practice with Sleep Makes Perfect:
1032 Sleep-Dependent Motor Skill Learning. *Neuron* **35**:205–211. doi:10.1016/S0896-6273(02)00746-
1033 8
- 1034 Wang T, Avraham G, Tsay JS, Abram SJ, Ivry RB. 2024a. Perturbation Variability Does Not Influence
1035 Implicit Sensorimotor Adaptation. *PLOS Computational Biology* **20**:e1011951.
1036 doi:10.1371/journal.pcbi.1011951
- 1037 Wang T, Avraham G, Tsay JS, Thummala T, Ivry RB. 2024b. Advanced feedback enhances sensorimotor
1038 adaptation. *Current Biology* **34**:1076-1085.e5. doi:10.1016/j.cub.2024.01.073
- 1039 Wang T, Ivry RB. 2023. A Cerebellar Population Coding Model for Sensorimotor Learning.
1040 doi:10.1101/2023.07.04.547720
- 1041 Wei K, Kording K. 2009. Relevance of Error: What Drives Motor Adaptation? *Journal of Neurophysiology*
1042 **101**:655–664. doi:10.1152/jn.90545.2008
- 1043 Yin C, Wei K. 2020. Savings in sensorimotor adaptation without an explicit strategy. *Journal of*
1044 *Neurophysiology* **123**:1180–1192. doi:10.1152/jn.00524.2019
- 1045 Zarahn E, Weston GD, Liang J, Mazzoni P, Krakauer JW. 2008. Explaining Savings for Visuomotor
1046 Adaptation: Linear Time-Invariant State-Space Models Are Not Sufficient. *Journal of*
1047 *Neurophysiology* **100**:2537–2548. doi:10.1152/jn.90529.2008
- 1048

1049 **Figure captions**

1050 **Fig 1. Experiment 1: Upon relearning a visuomotor rotation, implicit adaptation is**
1051 **attenuated.**

1052 **(A)** Task design and schematics of all trial types in Experiment 1. Using a trackpad or mouse,
1053 participants (N=44) moved a cursor from the start location (white circle) to a target (blue disk),
1054 with the target appearing at one of four locations (one representative location is depicted).
1055 There were 3 types of trials: 1) No feedback, with the cursor disappearing at movement onset;
1056 2) Veridical feedback, in which the direction of the cursor (small white disk) was veridical with
1057 respect to the direction of the movement; 3) Clamped feedback, in which the cursor followed an
1058 invariant path with respect to the target. **(B)** Top: Experimental protocol. The -C|CV|-C
1059 abbreviation indicates the main block-level structure of the experiment. There were two learning
1060 blocks with clamped feedback (-C), each followed by an aftereffect block with no feedback. To
1061 reset the sensorimotor map following the first learning block, we used a washout block
1062 composed of a reversed-clamp feedback phase (C) and a veridical feedback phase (V). The
1063 green oblique lines in the washout block mark the transition between the two phases, with the
1064 length of the reversed clamp phase determined on an individual basis (see Methods). Bottom:
1065 Time course of mean reach angle, with the data averaged within each cycle of four movements.
1066 Light and dark shading signify learning blocks 1 and 2, respectively, with the onset of the
1067 clamped feedback marked by the vertical solid lines. **(C)** Overlaid reach angle functions for the
1068 two learning blocks and two aftereffect blocks. Horizontal thick black lines denote clusters that
1069 show a significant difference between blocks 1 and 2 ($p < 0.05$). **(D)** The left panel (pair of bars)
1070 presents the aftereffect data (mean \pm SEM) for each learning block, measured as the averaged
1071 reach angle across all cycles in each aftereffect block. The right panel shows the within-
1072 participant difference (Aftereffect 2 – Aftereffect 1; dots and violin plot- distribution of individual

1073 difference scores, bar- mean difference and 95% CI). SEM, standard error of the mean. CI,
1074 Confidence Interval.

1075

1076 **Fig 2. Experiment 2: Implicit adaptation is not attenuated upon relearning when feedback**
1077 **is eliminated during the washout block.**

1078 (A) Experimental protocol and learning functions. Top: Participants (N=44) experienced 110
1079 cycles of trials without feedback (N) during a washout block that separated the two learning
1080 blocks (-C|N|-C design, purple). Bottom: Time course of mean reach angle averaged over
1081 cycles. Light and dark shading signify learning blocks 1 and 2, respectively, with the onset of the
1082 clamped feedback marked by the vertical solid lines. The design and learning functions from
1083 Experiment 1 are reproduced here to provide a visual point of comparison (gray). (B) Overlaid
1084 reach angle functions for the two learning blocks and two aftereffect blocks in Experiment 2
1085 (significant clusters based on $p < 0.05$) (C) The left panel presents the aftereffect (mean \pm SEM)
1086 for each learning block and the right panel the within-participant difference (Aftereffect 2 –
1087 Aftereffect 1; dots and violin plot- distribution of individual difference scores, bar- mean and 95%
1088 CI). (D) Scatter plot showing no relationship between the reach angle at late washout and
1089 change in relearning (Aftereffect 2 – Aftereffect 1). SEM, standard error of the mean. CI,
1090 Confidence Interval.

1091

1092 **Fig 3. Experiment 3: Attenuated adaptation does not require experience with salient,**
1093 **opposite signed error at the beginning of washout.**

1094 (A) Experimental protocol and learning functions. Top: At the beginning of the washout block in
1095 Experiment 3, participants (N=44) experienced a rotated cursor that was contingent on the
1096 direction of their hand movement, with the magnitude of the perturbation set to their final

1097 adaptation level at the end of the first learning block; in this way, the cursor position would be
1098 near the target. The size of the rotation was gradually decreased until reaching 0°, at which
1099 point it was veridical and remained so for the rest of the washout block (-C|R_eV|-C design,
1100 blue). Bottom: Time course of mean reach angle averaged over cycles (4 movements). Light
1101 and dark shading signify learning blocks 1 and 2, respectively, with the onset of the clamped
1102 feedback marked by the solid vertical lines. The design and learning functions from Experiment
1103 1 are reproduced here to provide a visual point of comparison (gray). **(B)** Distribution of errors
1104 experienced during the non-zero rotation phase of the washout block. These errors were small
1105 in magnitude (mean=2.9°, dark blue solid line) and in the opposite direction of the error
1106 experienced during the initial learning block (black solid line). Presumably, these opposite errors
1107 are the signals that drive the washout of the initial adaptation. The dotted line represents zero
1108 error. **(C)** Overlaid reach angle functions for the two learning blocks. Horizontal thick black lines
1109 denote clusters that show a significant difference between blocks 1 and 2 ($p < 0.05$). **(D)** The left
1110 panel presents the aftereffect (mean \pm SEM) for each learning block and the right panel the
1111 within-participant difference (Aftereffect 2 – Aftereffect 1; dots and violin plot- distribution of
1112 individual difference scores, bar- mean and 95% CI). SEM, standard error of the mean. CI,
1113 Confidence Interval.

1114

1115 **Fig 4. Experiment 4: Adaptation is attenuated for movements that were previously**
1116 **associated with either washout after learning or an extended baseline experience with**
1117 **veridical feedback.**

1118 **(A)** Experimental protocol and learning functions. Top: The target appeared at one of four
1119 locations, with two locations falling within one 30°-wedge and the other two falling within a
1120 same-size wedge on the opposite side of the workspace. Participants (N=44) experienced a -
1121 C|CV|-C schedule (cyan) in one wedge and a V₈₅-C design schedule in the other wedge

1122 (orange). For the latter, the number of veridical feedback cycles (85) matched the total number
1123 of cycles before relearning at the other wedge (excluding the no-feedback trials). Bottom: Time
1124 course of mean reach angle averaged over cycles, with each cycle consisting of 2 movements
1125 for each wedge. Light and dark cyan signify learning blocks 1 and 2 in the -C|CV|-C condition.
1126 (B) Overlaid reach angle functions comparing the first learning block in -C|CV|-C to that of the
1127 second learning block in the same wedge (left panel) and to the post long-baseline learning
1128 block at the other wedge (right panel). Horizontal thick black lines (B) and (C) denote clusters
1129 that show a significant difference between the functions (with $p < 0.017$ as a significance
1130 criterion, see Methods). (C) Left panel (bars) presents the aftereffect data (mean \pm SEM) for
1131 each learning block and the right panel shows the within-participant differences for three
1132 contrasts: 1) Aftereffect 2 – Aftereffect 1; 2) Aftereffect after long baseline – Aftereffect 1; 3)
1133 Aftereffect after long baseline – Aftereffect 2. Dots and violin plots show the distribution of
1134 individual difference scores; bar- mean and 95% CI. SEM, standard error of the mean. CI,
1135 Confidence Interval.

1136

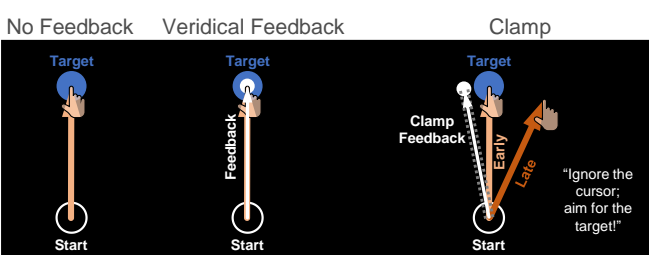
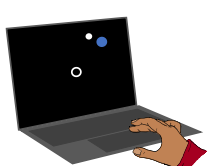
1137 **Fig 5. Experiment 5: Interference from veridical feedback is context-specific.**

1138 (A) Experimental protocol and learning functions. Top: During the learning block, participants
1139 ($N=60$) experienced rotated clamped feedback while reaching to six targets, with two targets
1140 falling within each of three wedges distributed across the workspace. For each wedge,
1141 participants experienced a different number of cycles with veridical feedback prior to the
1142 learning block: 5 (V_5 -C, light red); 45 (V_{45} -C, medium red); 85 (V_{85} -C, dark red). Bottom: Time
1143 course of mean reach angle averaged over cycles (2 movements) for each wedge. The vertical
1144 solid lines at cycles 45 and 85 mark the onset of movements to an additional location, and the
1145 vertical solid lines at cycles 90 mark the onset of the task-irrelevant clamped feedback.
1146 Horizontal thick black lines denote clusters of cycles that show a significant relationship

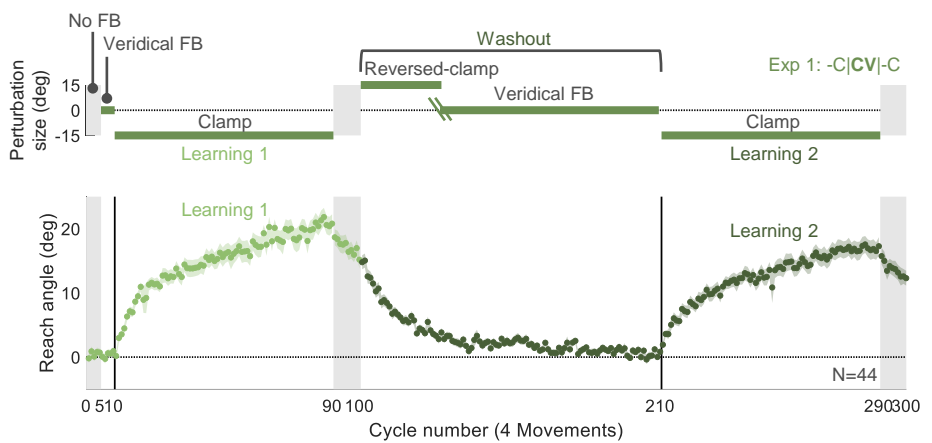
1147 between the reach angle and the number of veridical cycles ($p < 0.05$). **(B)** Left panel presents
1148 the aftereffect results (mean \pm SEM) for each learning condition with the fixed effect regression
1149 line obtained using a linear mixed model. Right panel shows the distribution (dots and violin
1150 plots) of individuals' slopes (random effect); bar- mean slope and 95% CI. SEM, standard error
1151 of the mean. CI, Confidence Interval.

Figure 1

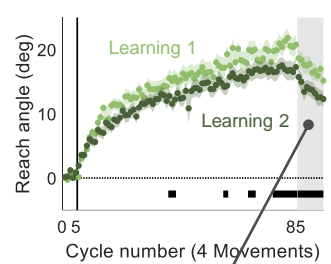
A



B



C



D

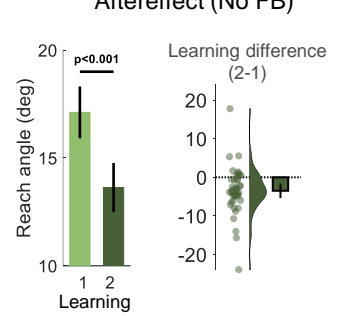
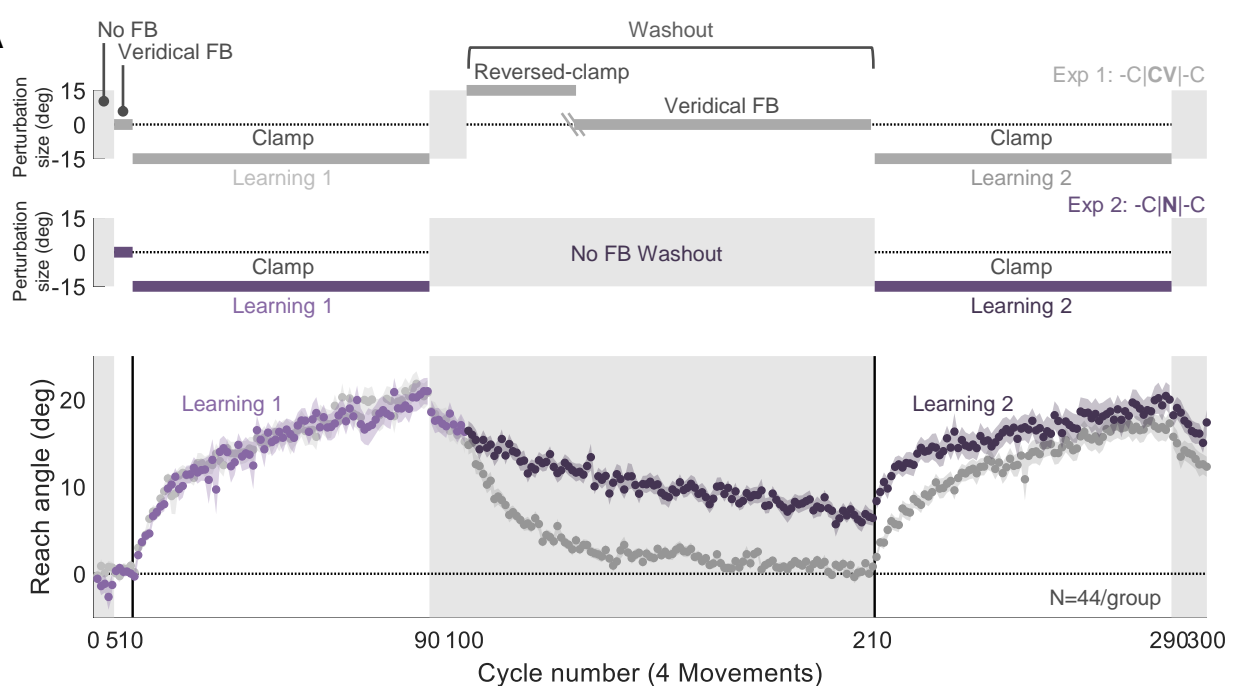
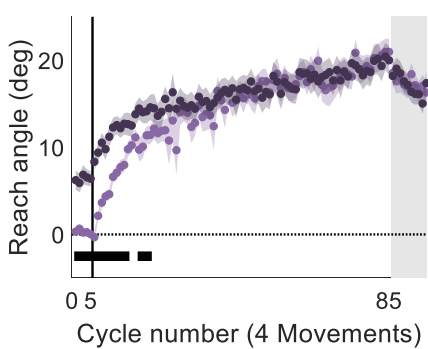


Figure 2

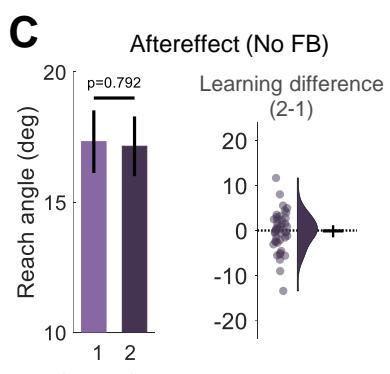
A



B



C



D

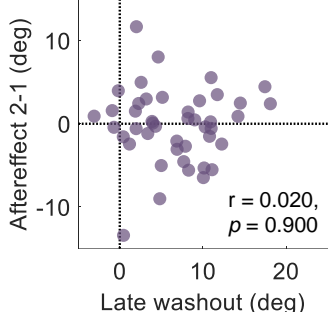


Figure 3

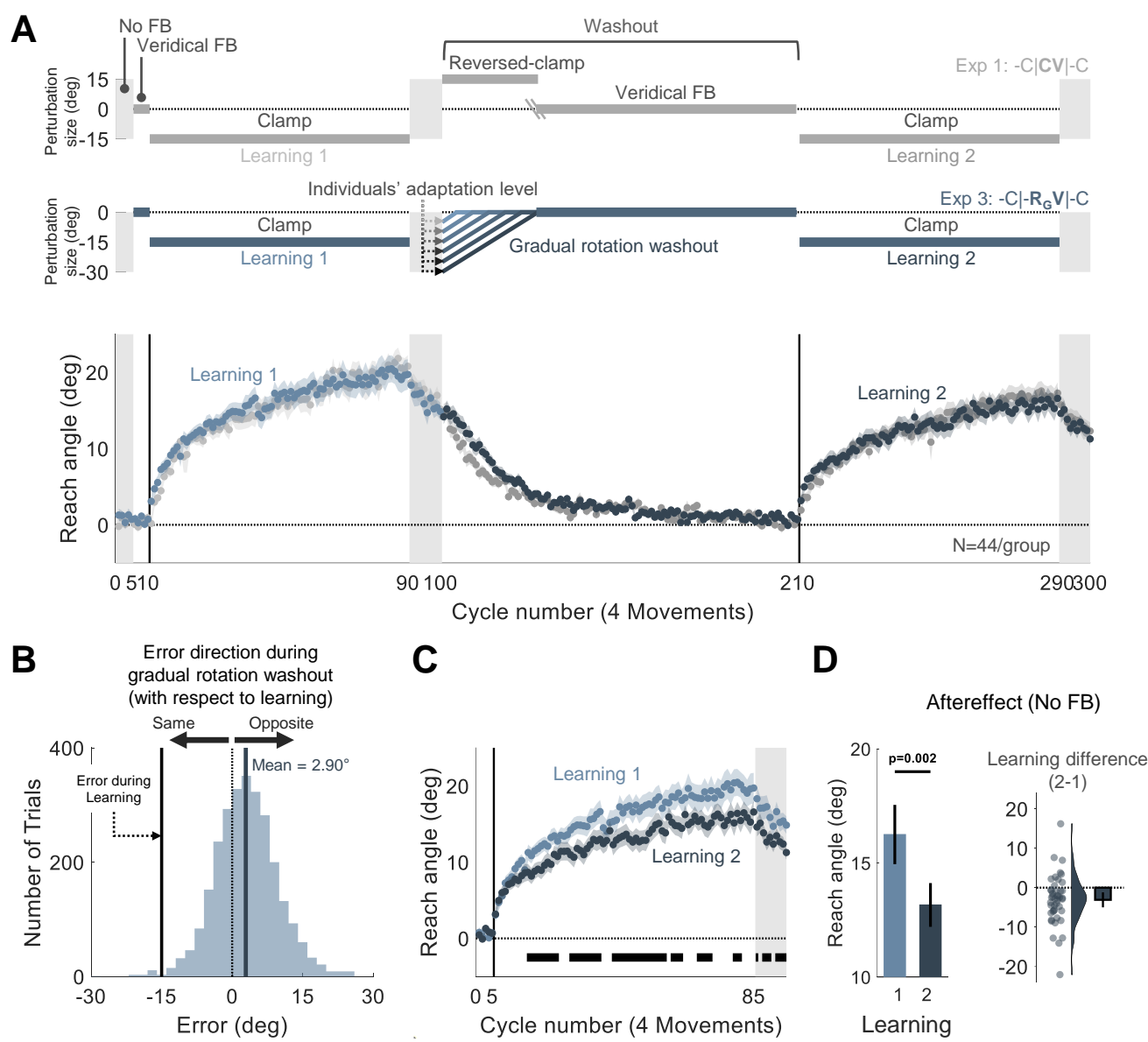


Figure 4

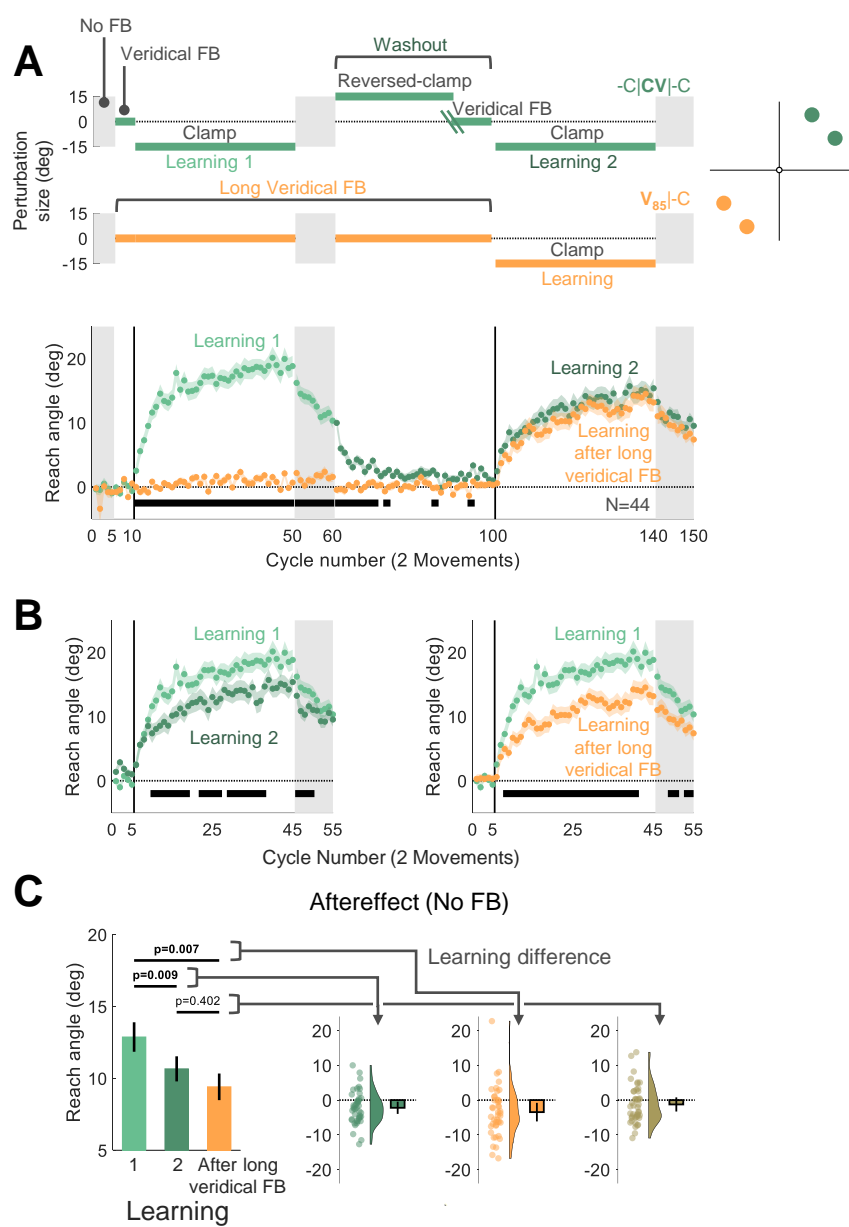
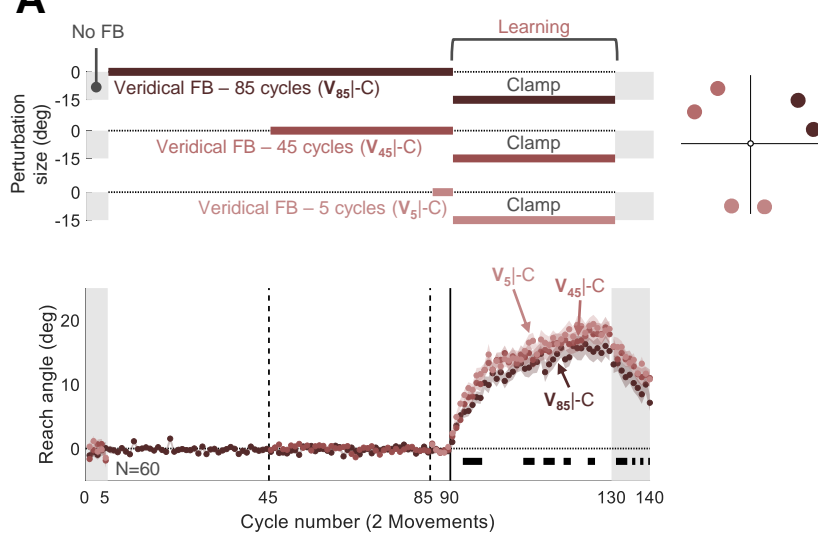


Figure 5

A



B

